

## Discovery of Clinical Candidate 4-[2-(5-Amino-1H-pyrazol-4-yl)-4-chlorophenoxy]-5-chloro-2-fluoro-N-1,3-thiazol-4-ylbenzenesulfonamide (PF-05089771): Design and Optimization of Diaryl Ether Aryl Sulfonamides as Selective Inhibitors of NaV1.7

Nigel Alan Swain, Dave Batchelor, Serge Beaudoin, Bruce M. Bechle, Paul A Bradley, Alan D Brown, Bruce Brown, Ken J Butcher, Richard P Butt, Mark L Chapman, Stephen Denton, David Ellis, Sebastien Galan, Stephen M Gaulier, Ben S Greener, Marcel J. de Groot, Mel S Glossop, Ian K Gurrell, Jo Hannam, Matthew S Johnson, Zhixin Lin, Christopher J Markworth, Brian E Marron, David S Millan, Shoko Nakagawa, Andy Pike, David Printzenhoff, David J Rawson, Sarah J Ransley, Steven M Reister, Kosuke Sasaki, R Ian Storer, Paul Anthony Stupple, and Christopher W West

*J. Med. Chem.*, **Just Accepted Manuscript** • DOI: 10.1021/acs.jmedchem.7b00598 • Publication Date (Web): 06 Jul 2017

Downloaded from <http://pubs.acs.org> on July 17, 2017

### Just Accepted

“Just Accepted” manuscripts have been peer-reviewed and accepted for publication. They are posted online prior to technical editing, formatting for publication and author proofing. The American Chemical Society provides “Just Accepted” as a free service to the research community to expedite the dissemination of scientific material as soon as possible after acceptance. “Just Accepted” manuscripts appear in full in PDF format accompanied by an HTML abstract. “Just Accepted” manuscripts have been fully peer reviewed, but should not be considered the official version of record. They are accessible to all readers and citable by the Digital Object Identifier (DOI®). “Just Accepted” is an optional service offered to authors. Therefore, the “Just Accepted” Web site may not include all articles that will be published in the journal. After a manuscript is technically edited and formatted, it will be removed from the “Just Accepted” Web site and published as an ASAP article. Note that technical editing may introduce minor changes to the manuscript text and/or graphics which could affect content, and all legal disclaimers and ethical guidelines that apply to the journal pertain. ACS cannot be held responsible for errors or consequences arising from the use of information contained in these “Just Accepted” manuscripts.



1  
2  
3  
4  
5  
6  
7  
8  
9  
10  
11  
12  
13  
14  
15  
16  
17  
18  
19  
20  
21  
22  
23  
24  
25  
26  
27  
28  
29  
30  
31  
32  
33  
34  
35  
36  
37  
38  
39  
40  
41  
42  
43  
44  
45  
46  
47  
48  
49  
50  
51  
52  
53  
54  
55  
56  
57  
58  
59  
60



SCHOLARONE™  
Manuscripts

1  
2  
3  
4  
5  
6  
7  
8  
9  
10  
11  
12  
13  
14  
15  
16  
17  
18  
19  
20  
21  
22  
23  
24  
25  
26  
27  
28  
29  
30  
31  
32  
33  
34  
35  
36  
37  
38  
39  
40  
41  
42  
43  
44  
45  
46  
47  
48  
49  
50  
51  
52  
53  
54  
55  
56  
57  
58  
59  
60

# Discovery of Clinical Candidate 4-[2-(5-Amino-1H-pyrazol-4-yl)-4-chlorophenoxy]-5-chloro-2-fluoro-N-1,3-thiazol-4-ylbenzenesulfonamide (PF-05089771): Design and Optimization of Diaryl Ether Aryl Sulfonamides as Selective Inhibitors of Na<sub>v</sub>1.7

*Nigel. A. Swain,<sup>\*,a,†</sup> Dave Batchelor,<sup>e</sup> Serge Beaudoin,<sup>d</sup> Bruce M. Bechle,<sup>c</sup> Paul A. Bradley,<sup>e</sup> Alan D. Brown,<sup>a</sup> Bruce Brown,<sup>e</sup> Ken J. Butcher,<sup>e</sup> Richard P. Butt,<sup>a</sup> Mark L Chapman,<sup>d</sup> Stephen Denton,<sup>e</sup> David Ellis,<sup>e</sup> Sebastien Galan,<sup>e</sup> Steven M. Gaulier,<sup>e</sup> Ben S. Greener,<sup>e</sup> Marcel J. de Groot,<sup>e</sup> Mel S. Glossop,<sup>e</sup> Ian K. Gurrell,<sup>f</sup> Jo Hannam,<sup>e</sup> Matthew S. Johnson,<sup>d</sup> Zhixin Lin,<sup>d</sup> Christopher J. Markworth,<sup>d</sup> Brian E. Marron,<sup>d</sup> David S. Millan,<sup>e</sup> Shoko Nakagawa,<sup>e</sup> Andy Pike,<sup>b,†</sup> David Printzenhoff,<sup>d</sup> David J. Rawson,<sup>e</sup> Sarah J. Ransley,<sup>e</sup> Steven M. Reister,<sup>d</sup> Kosuke Sasaki,<sup>e</sup> R. Ian Storer,<sup>a,†</sup> Paul A. Stupple,<sup>e</sup> Christopher W. West,<sup>d</sup>.*

<sup>a</sup>Worldwide Medicinal Chemistry, <sup>b</sup>Pharmacokinetics, Dynamics and Metabolism, Pfizer Ltd, The Portway, Granta Park, Cambridge, CB21 6GS, UK. <sup>c</sup>Worldwide Medicinal Chemistry, Pfizer Inc, Eastern Point Road, Groton, Connecticut 06340, USA. <sup>d</sup>Icagen Inc, 4222 Emperor Blvd # 350, Durham, NC 27703, USA. <sup>e</sup>Worldwide Medicinal Chemistry, <sup>f</sup>Pharmacokinetics, Dynamics and Metabolism, Pfizer Ltd, Ramsgate Road, Sandwich, Kent, CT13 9NJ, UK.

1  
2  
3 KEYWORDS. Na<sub>v</sub>1.7, pain, sodium channel, Na<sub>v</sub>1.5, CYP2C9 inhibition, microdose, aryl  
4  
5 sulfonamide  
6  
7

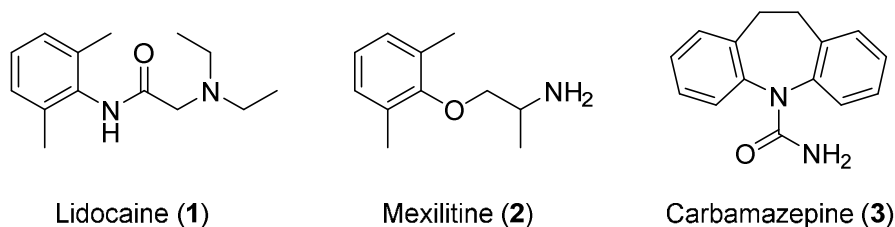
8  
9  
10 ABSTRACT

11  
12  
13 A series of acidic diaryl ether heterocyclic sulfonamides that are potent and sub-type selective  
14  
15 Na<sub>v</sub>1.7 inhibitors is described. Optimization of early lead matter focused on removal of  
16  
17 structural alerts, improving metabolic stability and reducing cytochrome P450 inhibition driven  
18  
19 drug-drug interaction concerns to deliver the desired balance of preclinical in vitro properties.  
20  
21 Concerns over non-metabolic routes of clearance, variable clearance in pre-clinical species and  
22  
23 subsequent low confidence human pharmacokinetic predictions led to the decision to conduct a  
24  
25 human microdose study to determine clinical pharmacokinetics. The design strategies and  
26  
27 results from pre-clinical PK and clinical human microdose PK data are described leading to the  
28  
29 discovery of the first sub-type selective Na<sub>v</sub>1.7 inhibitor clinical candidate PF-05089771 (**34**)  
30  
31 which binds to a site in the voltage sensing domain.  
32  
33  
34  
35  
36  
37

38  
39 INTRODUCTION

40  
41  
42 Voltage-gated sodium channels control the flow of sodium ions across cellular membranes and  
43  
44 are critical to the initiation and propagation of electrical impulses in excitable cells. There are  
45  
46 nine different human isoforms of sodium channels (Na<sub>v</sub>1.1-Na<sub>v</sub>1.9) with varying tissue  
47  
48 expression patterns in neurons, cardiac and skeletal muscle.<sup>1</sup> Several neuronally expressed  
49  
50 sodium channels have been linked to aberrant action potential firing associated with pain and  
51  
52 sodium channel inhibition has served as a point of pharmacological intervention in pain  
53  
54 management.<sup>2</sup> Indeed, non-selective Na<sub>v</sub> inhibitors such as lidocaine (**1**), mexilitine (**2**) and  
55  
56  
57  
58  
59  
60

1  
2  
3 carbamazepine (**3**) demonstrate clinical efficacy for chronic pain (Figure 1). However, these  
4  
5 agents are of limited clinical utility due to dose-limiting side effects associated with modulation  
6  
7 of non-pain-related  $\text{Na}_V$  sub-types.<sup>3</sup>  
8  
9



21 **Figure 1.** Selected examples of sodium channel inhibitors in clinical use.  
22  
23

24 Whilst several  $\text{Na}_V$  sub-types have been implicated as potential targets in reduction of pain the  
25 most compelling human genetic evidence indicates  $\text{Na}_V1.7$  as critical for pain perception.<sup>4</sup> Loss-  
26 of-function mutations in the *SCN9a* gene (which encodes  $\text{Na}_V1.7$ ) result in the rare genetic  
27 condition, congenital insensitivity to pain (CIP).<sup>5</sup> Conversely, gain-of-function mutations of  
28 *SCN9a* can lead to extreme pain conditions such as paroxysmal extreme pain disorder (PEPD)  
29 and peripheral erythromelalgia (PE).<sup>6</sup>  
30  
31  
32  
33  
34  
35  
36  
37  
38

39 This human genetic evidence has prompted the search for sub-type selective inhibitors of the  
40  $\text{Na}_V1.7$  channel as superior analgesics with a significantly reduced side-effect burden compared  
41 with pan- $\text{Na}_V$  blockade.<sup>7</sup>  
42  
43  
44  
45  
46

47 We pioneered work which identified novel lead matter containing an aryl sulfonamide acid  
48 isostere with superior sub-type selectivity particularly over the cardiac channel  $\text{Na}_V1.5$   
49 (inhibition of which may lead to arrhythmias).<sup>8</sup> Elegant mutagenesis studies suggested  
50 molecules such as **5** (PF-04856264) bind to a unique site in the voltage sensor domain IV which  
51 is distinct from the local anesthetic and tetrodotoxin (**4**) pore binding sites (Figure 2).<sup>9</sup> The  
52  
53  
54  
55  
56  
57  
58  
59  
60

existence of this novel binding site has recently been confirmed by a X-ray crystal structure of a chimeric human  $\text{Na}_v1.7$  voltage sensor domain IV in complex with an aryl sulfonamide.<sup>10</sup>

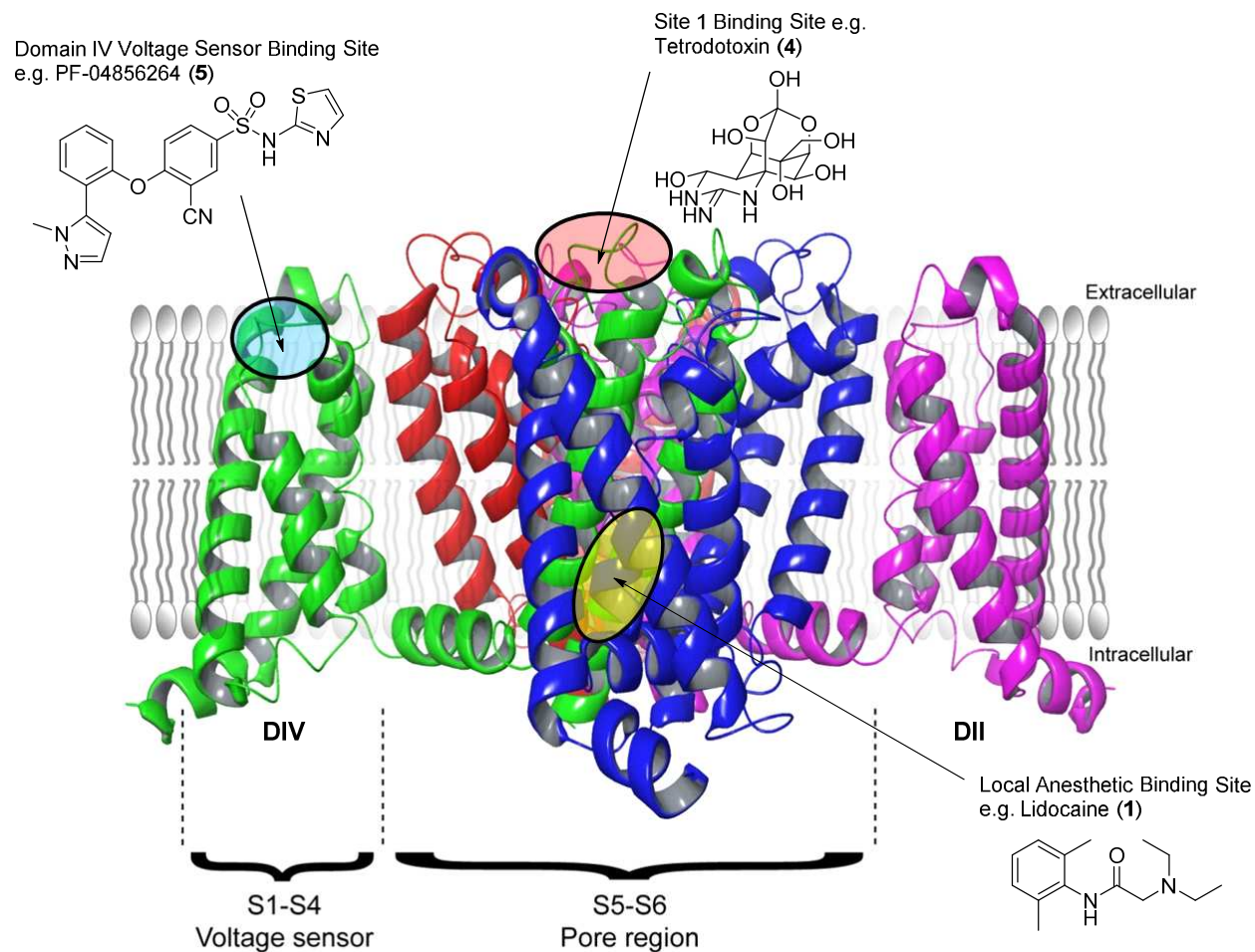


**Figure 2.** Transmembrane view of sodium channel from the bacterium *Arcobacter butzleri* ( $\text{Na}_v\text{Ab}$  PDB code 3RVY)<sup>11</sup> Domains DI-IV are represented in different colors (DI – red, DII – magenta, DIII – blue, DIV – green). The postulated binding sites are highlighted for local anesthetics (yellow), tetrodotoxin (red) and acidic aryl sulfonamides (blue).

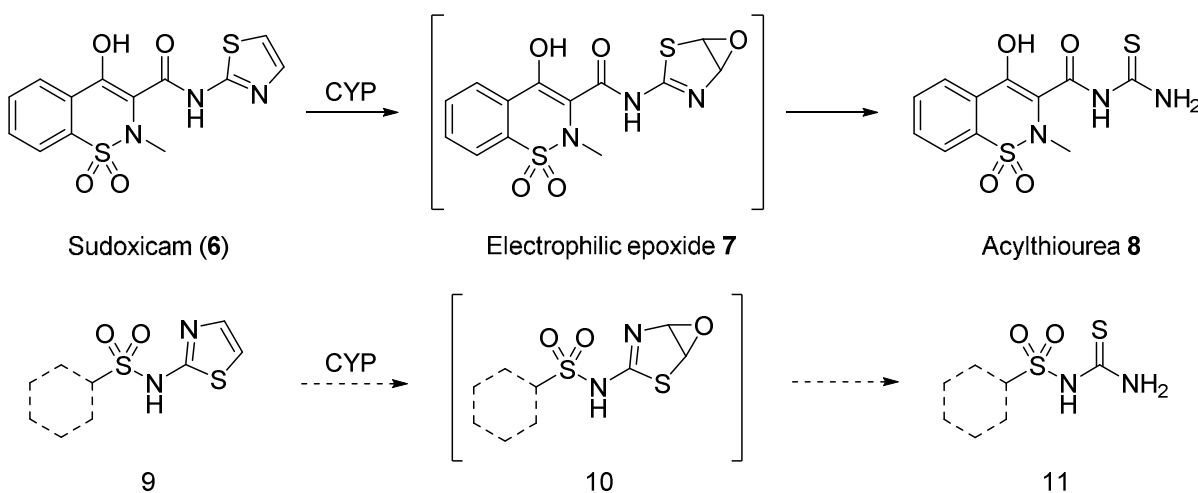
Many groups have subsequently actively targeted this novel binding site which offers enhanced sub-type selectivity over traditional non-selective pore region binding ligands.<sup>12</sup> However, this

has presented many medicinal chemistry and development challenges associated with progression of high molecular weight, lipophilic, acidic small molecules.

Herein we report the work that resulted in the discovery and optimization of a series of acidic diaryl ether aryl sulphonamides leading to the delivery of a clinical candidate with enhanced sub-type selectivity vs known agents.

## RESULTS AND DISCUSSION

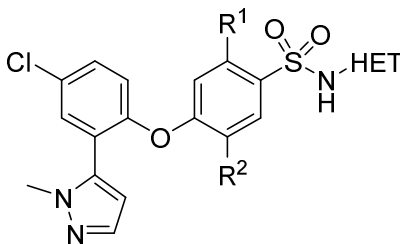
Initial work focused on replacement of the 2-amino thiazole moiety from early leads such as compound **5** to mitigate the risk of idiosyncratic drug toxicity. The risk associated with a 2-amino thiazole group is exemplified by Sudoxicam (**6**) which was removed from Phase III clinical trials due to hepatotoxicity. Its suspension has been attributed to cytochrome P450 mediated ring oxidation to an electrophilic epoxide **7** (Figure 3).<sup>13</sup> Subsequent hydrolytic ring scission yields acylthiourea metabolite **8** capable of oxidizing glutathione and proteins. Therefore, we sought suitable replacements for this known structural alert whereby the 2-sulfonamido linked thiazoles **9** had the potential to undergo a similar metabolic fate as **6** to reveal both reactive epoxide intermediates **10** and potentially hepatotoxic sulfonylthiourea adducts **11**.

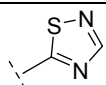
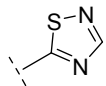
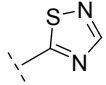


**Figure 3.** Metabolic pathway of hepatotoxin Sudoxicam (**6**) and implication for acidic 2-amino thiazole containing aryl sulfonamide Na<sub>v</sub>1.7 series.

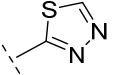
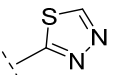
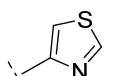
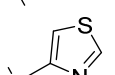
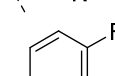
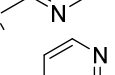
Replacement of the 2-aminothiazole with a number of other 5 and 6 membered heterocycles (**12-20**) was successful in maintaining good to excellent levels of hNa<sub>v</sub>1.7 activity whilst maintaining high levels of Na<sub>v</sub>1.5 selectivity (Table 1). Furthermore, these alternative heterocycles eliminated the potential for thiourea adducts formation resulting from cytochrome P450 (CYP) mediated ring oxidation. Incorporation of an additional nitrogen atom into the thiazole ring provided more acidic 1,2,4-thiadiazole analogues **12-14** (pK<sub>a</sub>'s ~3.5) and 1,3,4-thiadiazole regioisomers **15-16** (pK<sub>a</sub>'s ~4.5) which demonstrated high lipophilic efficiency (LipE) and selectivity over hNa<sub>v</sub>1.5.

**Table 1.** Selected SAR of core substitution and heterocyclic RHS<sup>a</sup>



	R <sup>1</sup> , R <sup>2</sup>	HET	clogD <sup>b</sup>	hNa <sub>v</sub> 1.7 IC <sub>50</sub> (nM) <sup>c</sup>	hNa <sub>v</sub> 1.5 IC <sub>50</sub> (nM) <sup>c</sup>	HLM CL <sub>int</sub> , app (μL/min/ mg)	CYP3A4 IC <sub>50</sub> (nM)	CYP2C9 IC <sub>50</sub> (nM)	LipE <sup>d</sup>
<b>12</b>	H, CN		0.9	21	>30000	92	556	517	6.8
<b>13</b>	H, F		1.2	31	15060	>262	N.D.	N.D.	6.3
<b>14</b>	F, F		1.2	5	22210	>320	<30	39	7.1



15	H, CN		0.5	244	25448	68	N.D.	N.D.	6.1
16	F, Cl		1.2	20	>30000	>300	11068	100	6.5
17	H, CN		1.8	465	>10000	65	>30000	1368	4.5
18	F, Cl		2.2	34	25786	229	26588	37	5.3
19	F, Cl		2.9	57	>10000	>320	N.D.	N.D.	4.3
20	F, Cl		1.5	30	>10000	90	1058	184	6.0

<sup>a</sup>N.D. = not determined. <sup>b</sup>clogD calculated logD based on shake-flask method in octanol and water at pH<sub>7.4</sub>. <sup>c</sup>V<sub>half</sub> inactivation protocol using PatchXpress™ platform (mean IC<sub>50</sub> >2 replicates). <sup>d</sup>LipE = -logIC<sub>50</sub> - clogD.

Interestingly the 4-thiazole analogue in combination with a nitrile core **17** lost significant LipE although this could be regained by core substituent replacement to the more lipophilic F/Cl analogue **18**. Pleasingly 6-membered heterocyclic replacements such as fluoro-pyridyl **19** and pyrimidyl **20** were also tolerated in combination with F/Cl core substituents although were not as efficient as their thiazole counterparts. However, all these molecules suffered from high human liver microsome (HLM) clearance with N-demethylation of the LHS pyrazole group confirmed as the major metabolite in metabolite identification studies. Furthermore, we were concerned by significant inhibition of the CYP isoforms 3A4 and 2C9.

**Table 2.** Broader Nav pharmacology profile for compounds **12** and **13**.<sup>a</sup>

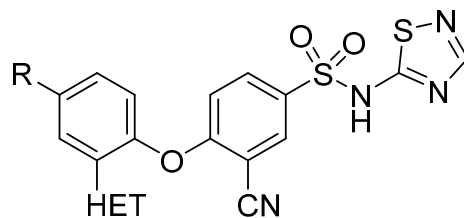
	<b>12</b>	<b>13</b>
hNav1.1 IC <sub>50</sub> (nM)	>3000	216

hNa <sub>v</sub> 1.2 IC <sub>50</sub> (nM)	276	149
hNa <sub>v</sub> 1.3 IC <sub>50</sub> (nM)	>3000	292
hNa <sub>v</sub> 1.5 IC <sub>50</sub> (nM)	>30000	15060
hNa <sub>v</sub> 1.6 IC <sub>50</sub> (nM)	199	510
hNa <sub>v</sub> 1.7 IC <sub>50</sub> (nM)	21	31
hNa <sub>v</sub> 1.8 IC <sub>50</sub> (nM)	>10000	>3000
rNa <sub>v</sub> 1.7 IC <sub>50</sub> (nM)	813	124

<sup>a</sup>V<sub>half</sub> inactivation protocols using PatchXpress™ platform.<sup>14</sup>

Intriguingly, core substitution changes at R<sup>2</sup> imparted a dramatic effect on the sub-type and orthologue selectivity as demonstrated by a broader Na<sub>v</sub> pharmacology profiling of matched pairs **12** and **13** (Table 2). With the exception of hNa<sub>v</sub>1.6 the selectivity window for nitrile core analogue **12** was superior to its fluoro partner **13**, particularly hNa<sub>v</sub>1.1 (>140x vs 7x respectively) and hNa<sub>v</sub>1.3 (>140x vs 9x respectively). Furthermore, a shift in the rat Na<sub>v</sub>1.7 activity was noted (39x vs 4x for compounds **12** and **13** respectively) which remained a key consideration in selecting molecules for in vivo evaluation throughout the drug discovery campaign. The excellent LipE and Na<sub>v</sub> sub-type selectivity profile of the 1,2,4-thiadiazole in combination with a nitrile R<sup>2</sup> substituent (as represented by compound **12**) became the focus and we turned our attention to solving the HLM and CYP inhibition liabilities through modifications to the pendant ortho-substituted heterocycle (Table 3).

**Table 3.** Selected SAR of ortho-substituted phenyl substitution



	R	HET	logD <sup>a</sup>	hNav1.7 IC <sub>50</sub> <sup>b</sup> (nM)	hNav1.5 IC <sub>50</sub> <sup>b</sup> (nM)	HLM CL <sub>int, app</sub> (μL/min/ mg)	CYP3A4 IC <sub>50</sub> (nM)	CYP2C9 IC <sub>50</sub> (nM)	LipE <sup>c</sup>
21	Cl		1.6	30	25231	22	400	205	5.9
22	Cl		1.7	4	17060	17	505	83	6.7
23	CF <sub>3</sub>		2.0	2	11102	28	737	372	6.7
24	Cl		1.0	11	>10000	<8	827	894	7.0
25	Cl		1.6	9	>10000	39	205	279	6.4
26	CF <sub>3</sub>		0.9	325	25578	39	910	180	5.6
27	CF <sub>3</sub>		0.7	324	43699	19	616	321	5.8
28	CF <sub>3</sub>		0.7	13	35118	14	1271	2200	7.2

<sup>a</sup>logD measured via shake-flask method in octanol and water at pH<sub>7.4</sub>. <sup>b</sup>V<sub>half</sub> inactivation protocol using PatchXpress™ platform.<sup>14</sup>  
<sup>c</sup>LipE=-logIC<sub>50</sub>-logD.

Des-methyl analogue **21** significantly increased metabolic stability in HLM compared to parent molecule **12** whilst symmetrical pyrazole derivative **22** further increased LipE in combination with low HLM. However, both analogues continued to suffer from high CYP2C9 inhibition (7x and 20x for compounds **21** and **22** respectively) giving the potential for a significant drug-drug

interaction (DDI). To aid design of molecules with reduced CYP2C9 inhibition liability we extended our studies to explore co-crystallization of our Na<sub>v</sub>1.7 aryl sulfonamides in CYP2C9. Pleasingly, we were able to solve a crystal structure of a related 2-aminothiazole analogue **29** in complex with CYP2C9 (Figure 4). Critically, the RHS acidic moiety interacts with a key Arg108 residue orientating the LHS of the ligand towards the heme region. In this case the pyrazole forms T-stacking and N-donor interactions with the iron complex. Given the RHS acidic heterocyclic sulfonamide group was a crucial pharmacophore for Na<sub>v</sub>1.7 inhibition our strategy to decrease CYP2C9 inhibition was to disrupt the hemo interaction through steric and/or electronic modifications to the pendent LHS heterocycle.

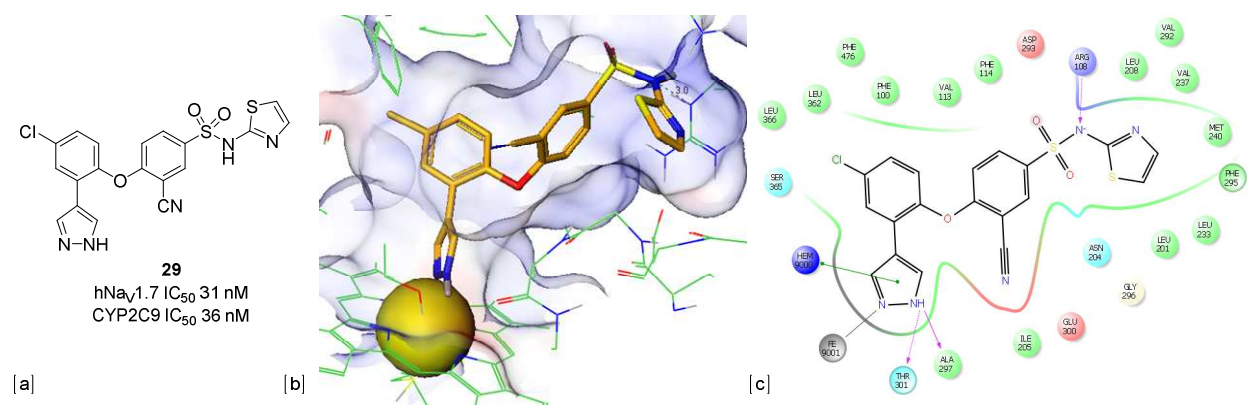


**Figure 4.** (a) Structure and profile of 2-aminothiazole analogue **29**. (b) X-ray crystal structure of **29** in complex with CYP2C9 (PDB code 5K7K). Iron atom shown as a yellow sphere. (c) Key interactions between **29** and CYP2C9. Pink arrows indicate H-bond interactions with the protein (dotted lines indicate interactions with sidechains and filled lines indicate interactions with the backbone). Green arrows indicate stacking interactions while brown arrows indicate other contacts (in this case, the interaction with Fe<sup>2+</sup>). Residues are colored by type: red are acidic residues; green are hydrophobic residues; cyan are polar residues and blue are basic residues.

1  
2  
3 Based on this hypothesis, substitution of the pyrazole group with either a methyl or amino group  
4 provided potent, selective and high LipE ligands **23** and **24** respectively. Both compounds also  
5 demonstrated a significant improvement in CYP2C9 selectivity (186x and 81x for compounds **23**  
6 and **24** respectively) likely due to unfavorable interactions with the protein. Conversely, six-  
7 membered heterocycles proved more challenging replacements to boost the CYP2C9 selectivity  
8 window. Amino-pyridine **25** showed no improvement in CYP selectivity and diazole analogues  
9 such as pyrimidine **26** and pyridazine **27** eroded  $\text{Na}_v1.7$  activities with concomitant shift in LipE  
10 independent from CYP2C9 activity resulting in no selectivity. However, symmetrical pyridazine  
11 analogue **28** provided an excellent balance of primary activity, sub-type selectivity and  
12 lipophilicity in combination with reduced CYP liability (169x for 2C9 and 98x for 3A4) in one  
13 of the most efficient molecules synthesized on the project (LipE = 7.2). The significant  
14 reduction in CYP2C9 inhibition for pyridazine **28** was not expected and is a clear outlier from  
15 related unsubstituted 6-membered heterocyclic ring systems. We hypothesized that the unusual  
16 adjacent dual lone pair system of the pyridazine nitrogens form unfavorable interactions with the  
17 heme region of CYP2C9. Unfortunately, attempts to better understand these interactions via co-  
18 crystallization of pyridazine containing analogues in CYP2C9 failed.

19  
20  
21  
22  
23  
24  
25  
26  
27  
28  
29  
30  
31  
32  
33  
34  
35  
36  
37  
38  
39  
40  
41 Several lead compounds possessing the 1,2,4-thiadiazole RHS with high LipE (>6.5) and low  
42 intrinsic clearance (<30  $\mu\text{L}/\text{min}/\text{mg}$ ) in pre-clinical species were evaluated in pharmacokinetic  
43 (PK) studies (Table 4). Following intravenous (IV) dosing of pyrazole derivatives **22** and **23** in  
44 rats and dogs much higher plasma clearances were observed compared to their corresponding  
45 scaled in vitro microsomal  $\text{Cl}_{\text{int}}$  measurements suggesting a significant contribution from non-  
46 metabolic clearance pathway(s). Oral dosing in rat for compound **23** and dog for compound **22**  
47 also demonstrated low bioavailability consistent with a contribution from incomplete absorption  
48  
49  
50  
51  
52  
53  
54  
55  
56  
57  
58  
59  
60

1  
2  
3 which we attributed, based on data from the RRCK assay, to low passive permeability for these  
4 high TPSA, acidic (pKa ~3.5) molecules. Despite its reduced lipophilicity, pyridazine analogue  
5  
6 **28** also showed very high clearance in rat and moderate clearance in dog. Following IV  
7  
8 administration of **28** to bile duct cannulated rats ~73% of the dose was excreted in bile as  
9  
10 unchanged drug during the 6 hour study suggesting the high clearance was non-metabolic. Early  
11  
12 PK work with this chemotype also confirmed our hypothesis that molecules in this  
13  
14 physicochemical space (high MW, high TPSA, acids) demonstrate very low levels of CNS  
15  
16 exposure. Given Nav1.7 is highly expressed in peripheral sensory neurons we rationalized only  
17  
18 peripheral block of Nav1.7 was required for efficacy and that limiting CNS penetration would be  
19  
20 desirable to further reduce centrally mediated toxicity effects (e.g. via inhibition of Nav1.1 and  
21  
22 Nav1.2).  
23  
24  
25  
26  
27  
28  
29  
30  
31

32 **Table 4.** Physicochemical, in vitro ADME and pre-clinical pharmacokinetic profiles for lead  
33 1,3,4-thiadiazoles.<sup>a</sup>  
34  
35

Compound	<b>22</b>	<b>23</b>	<b>28</b>
<b>Physicochemical properties</b>			
MW (Da)	458	506	504
clogP	2.8	3.2	2.2
logD <sub>7.4</sub>	1.7	2.0	0.7
TPSA (Å) <sup>2</sup>	134	134	131
Solubility at pH6.5 (μM)	259	>300	>300

<b>ADME in vitro profile</b>						
RRCK ( $\times 10^{-6}$ cm/sec)	2.1		1.1		0.7	
HLM/RLM/DLM, Clint ( $\mu\text{L}/\text{min}/\text{mg}$ )	17 / 26 / <5		28 / 29 / 9		14 / 23 / <5	
Hhep, Rheps, DHeaps Clint ( $\mu\text{L}/\text{min}/10^6$ cells)	18 / 5 / N.D.		34 / N.D./N.D.		7 / 11 / N.D.	
hPPB, rPPB, dPPB (Fu)	<0.001, 0.0022, 0.0022		0.0015, 0.0043, 0.0039		0.00543, 0.015, 0.021	
<b>in vivo PK</b>	Rat	Dog	Rat	Dog	Rat	Dog
IV dose (mg/kg)	1	0.1	1	0.1	1	0.1
$Cl_p$ (mL/min/kg)	43	6.5	40.1	21.2	58.0	10.0
$Cl_u$ (mL/min/kg)	19545	2955	9325	5435	3866	476
$V_{ss}$ (L/kg)	2.3	0.5	6.3	1.8	1.3	1.2
$T_{1/2}$ (h)	<1	0.9	5.1	1.2	0.2	3.1
Oral dose (mg/kg)	N.D.	0.13	3	N.D.	3	N.D.
$C_{max}$ (ng/mL)		18	4		1	
$AUC_{0 \rightarrow \infty}$ (ng*h/mL)		40	26		5	
F (%)		23	<5		<1	

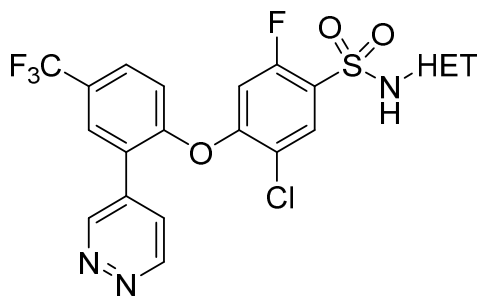
<sup>a</sup>N.D. = not determined.

Several LHS substituents had now been identified which were optimized for LipE, metabolic stability and CYP2C9 selectivity. Subsequent designs to re-explore the core substituents and alternative heterocyclic RHS groups were initiated in an attempt to reduce the TPSA and acidity

and explore the impact on pre-clinical clearance and oral absorption. Furthermore, earlier evidence (as observed with representatives in Table 1) also suggested alternative non-1,2,4-thiadiazole heterocycles could offer improvements in the selectivity over CYP3A4 inhibition, reducing any associated DDI risk.

Utilizing pyridazine **28** as an advanced lead the nitrile core was switched to the lower TPSA expressing F/Cl substitution pattern and less acidic RHS heterocyclic alternatives were synthesized (Table 5). 1,3,4-Thiadiazole derivative **30** (measured pKa 4.0) maintained high LipE and improved HLM  $CL_{int}$  and CYP3A4 selectivity (536x) over compound **28**. The 4-thiazole derivative **31** (estimated pKa 5.6) also showed reduced CYP3A4 liability although this more lipophilic expression showed moderate turnover in HLM and reduced LipE.

**Table 5.** Heterocyclic changes with an optimized pyridazyl LHS



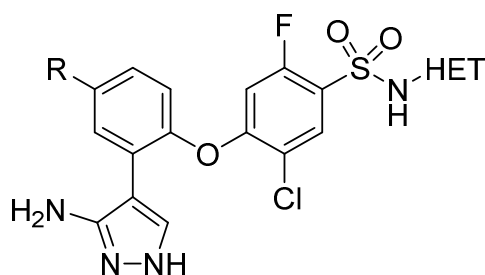
HET	logD <sup>a</sup>	TPSA	hNav1.7 IC <sub>50</sub> (nM) <sup>b</sup>	hNav1.5 IC <sub>50</sub> (nM) <sup>b</sup>	HLM CL <sub>int, app</sub> (μL/min/ mg)	CYP3A4 IC <sub>50</sub> (nM)	CYP2C9 IC <sub>50</sub> (nM)	LipE <sup>c</sup>
<b>30</b>	0.8	107	21	>30000	<8	>11248	1101	6.9
<b>31</b>	1.6	94	26	22451	17	>30000	1365	6.0

<sup>a</sup>logD measured via shake-flask method in octanol and water at pH<sub>7.4</sub>. <sup>b</sup>V<sub>half</sub> inactivation protocol using PatchXpress™ platform.<sup>14</sup>  
<sup>c</sup>LipE=-logIC<sub>50</sub>-logD.



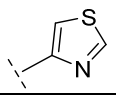
The high LipE and improved CYP2C9 profile for amino-pyrazole example **24** (Table 3) was intriguing although the high TPSA and HBD/HBA expression of this LHS moiety led to significant concerns over oral absorption. However, an exploration of alternative RHS expressions with the lower TPSA expressing F/Cl core was undertaken providing 1,3,4-thiadiazole and 4-thiazole derivatives **32-34**, all showing an improved CYP3A4 selectivity window whilst maintaining good levels of Nav1.7 activity (Table 6). Unfortunately, following a 3 mg/kg oral administration of high LipE thiadiazole **32** in rat, oral bioavailability was calculated to be <5 % (despite clearance approximately 25% liver blood flow) suggesting poor absorption with this high TPSA, moderately acidic (measured acidic pKa 4.3) example. However, the lower TPSA and weakly acidic 4-thiazole derivatives **33** and **34** (measured acidic pKa 6.3) both demonstrated good oral bioavailability in rat and a PK summary for compound **34** is provided in table 8 and will be discussed in more detail later in this manuscript.

**Table 6.** Heterocyclic changes with an optimized amino-pyrazole LHS



	R	HET	logD <sup>a</sup>	TPSA	hNav1.7 IC <sub>50</sub> (nM) <sup>b</sup>	hNav1.5 IC <sub>50</sub> (nM) <sup>b</sup>	HLM CL <sub>int</sub> , app (μL/min/mg)	CYP3A 4 IC <sub>50</sub> (nM)	CYP2C9 IC <sub>50</sub> (nM)	LipE <sup>c</sup>
<b>32</b>	CF <sub>3</sub>		0.9	136	8	14413	<9	>30000	658	7.2
<b>33</b>	CF <sub>3</sub>		2.2	123	9	10549	<9	>30000	552	5.8

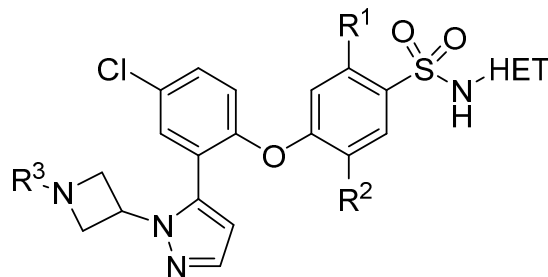
1  
2  
3  
4  
5  
6  
7  
8  
9  
10  
11  
12  
13  
14  
15  
16  
17  
18  
19  
20  
21  
22  
23  
24  
25  
26  
27  
28  
29  
30  
31  
32  
33  
34  
35  
36  
37  
38  
39  
40  
41  
42  
43  
44  
45  
46  
47  
48  
49  
50  
51  
52  
53  
54  
55  
56  
57  
58  
59  
60

34	Cl		2.3	123	11	>10000	10	>30000	299	5.5
----	----	---	-----	-----	----	--------	----	--------	-----	-----

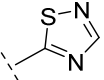
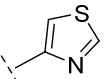
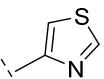
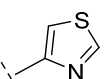
<sup>a</sup>logD measured via shake-flask method in octanol and water at pH<sub>7.4</sub>. <sup>b</sup>V<sub>half</sub> inactivation protocol using PatchXpress™ platform.<sup>14</sup>  
<sup>c</sup>LipE=-logIC<sub>50</sub>-logD.

During the course of our SAR studies we identified that zwitterionic ligands (via incorporation of a basic center distal to the key acidic pharmacophore) were also well tolerated as hNav<sub>1.7</sub> inhibitors. Alkylated azetidines substituted pyrazoles **35-38** provided molecules with good levels of Nav<sub>1.7</sub> activity and excellent selectivity against Nav<sub>1.5</sub> (Table 7). Unfortunately PK profiling of 1,2,4-thiadiazole analogue **35** resulted in liver blood flow clearance in rat thwarting any desire to progress further. Pleasingly, 4-thiazole analogues **36-38** provided higher selectivity windows over CYP inhibition. Furthermore, increasing the size of the R<sup>3</sup> alkyl group from a methyl in example **37** to ethyl analogue **38** was not detrimental to Nav<sub>1.7</sub> activity or metabolic stability in HLM and continued to widen the CYP inhibition window. Interesting, despite its lower LipE, nitrile core example **36** showed impressive levels of Nav<sub>v</sub> sub-type selectivity (see table 8 for full pharmacology profile) consistent with earlier observations for the 1,3,4-thiadiazole, nitrile core acidic molecules.

**Table 7.** Optimization of zwitterionic substrate



R <sup>1</sup> , R <sup>2</sup>	R <sup>3</sup>	HET	logD <sup>a</sup>	TPSA	hNav <sub>1.7</sub> IC <sub>50</sub> (nM) <sup>b</sup>	hNav <sub>1.5</sub> IC <sub>50</sub> (nM) <sup>b</sup>	HLM CL <sub>int, app</sub> (μL/min/ mg)	CYP3A4 IC <sub>50</sub> (nM)	CYP2C9 IC <sub>50</sub> (nM)	LipE <sup>c</sup>
---------------------------------	----------------	-----	-------------------	------	---	---	--	---------------------------------	---------------------------------	-------------------

35	F, F	Me		1.0	102	3	29291	N.D.	427	264	7.5
36	H, CN	Et		1.4	113	46	>30000	13	12239	17992	5.9
37	F, F	Me		1.3	89	7	>30000	27	15124	1012	6.8
38	F, F	Et		1.6	89	10	>10000	25	>30000	3234	6.4

<sup>a</sup>logD measured via shake-flask method in octanol and water at pH<sub>7.4</sub>. <sup>b</sup>V<sub>half</sub> inactivation protocol using PatchXpress™ platform.<sup>14</sup>  
<sup>c</sup>LipE=-logIC<sub>50</sub>-logD.

More extensive analysis of three advanced molecules (examples **30**, **34** and **36**) with superior in vitro ADME and primary pharmacology profiles was carried out (Table 8). Upon full Nav pharmacology profiling excellent sub-type selectivities were confirmed together with a general shift in the orthologue activity which was most pronounced in rat. Compounds **30**, **34** and **36** were also tested for off-target pharmacology against a broad range of receptors, enzymes and ion channels at CEREP (Bioprint) and within Pfizer (see SI). Encouragingly, a low perceived safety risk was posed by the levels of activity observed in these selectivity panels.

Generally within the series the preclinical in vivo PK was not reliably predicted by in vitro metabolic Cl<sub>int</sub> using appropriate liver microsomes or hepatocyte systems. It was also notable that there were distinct trends in PK between species with rats typically displaying high clearance and atypical PK profiles for acidic molecules, such as high V<sub>ss</sub>, while dogs typically showed lower clearance and more typical PK.<sup>15</sup> Various pieces of in vitro data, including Sandwich Cultured Human Hepatocytes (data not shown) and OATP expressing cell lines, suggested a potential contribution to clearance from active hepatic uptake. It was also noted in bile duct cannulated rat studies that these compounds showed significant contributions from

biliary clearance of unchanged drug, although the relevance to other species was not well understood.

The failure of in vitro scaling to predict preclinical PK, inconsistent preclinical PK between species, and data suggesting the potential for a significant contribution from non-metabolic clearance routes, raised significant concerns of the likely accuracy of human PK predictions for compounds in this series. Therefore, these three compounds from the diaryl ether aryl sulfonamides series described, **30**, **34** and **36**, were chosen for inclusion in a human microdose study, where the PK profiles were determined following intravenous and oral administration.<sup>16</sup>

A fourth compound from an alternative indazole series was also included in the microdose study and will be the topic of future disclosures. It is noteworthy that whilst LipE proved a key parameter in ligand design to improve overall physicochemical properties for the series, compounds **34** and **36** display some of the lowest LipEs reported for our most advanced inhibitors. This is a reflection of the major challenges faced with this chemotype to deliver structurally differentiated molecules for a human microdose study balancing low DDI risk, high oral absorption and acceptable pre-clinical clearance.

**Table 8.** Physicochemical properties, in vitro ADME, Na<sub>v</sub> pharmacology and pre-clinical pharmacokinetic profiles for lead microdose molecules.<sup>a</sup>

Compound	<b>30</b>	<b>34</b>	<b>36</b>
<b>Physicochemical properties</b>			
MW (Da)	532	500	541
clogP	3.1	4.2	4.4
logD <sub>7.4</sub>	0.9	2.6	1.4
pK <sub>a</sub> acid, [base]	4.3	6.3	6.5 [7.4]

TPSA ( $\text{\AA}^2$ )	107	123	113			
Solubility at pH6.5 ( $\mu\text{M}$ )	286	<0.3	>262			
<b>ADME in vitro profile</b>						
RRCK ( $\times 10^{-6}$ cm/sec)	0.7	3.8	3.2			
MDCK-MDR1 $P_{\text{app}}$ AB/BA ( $\times 10^{-6}$ cm/sec)	<0.5/1.1	0.7/6.3	<0.5/11			
HLM/RLM/DLM, $Cl_{\text{int}}$ ( $\mu\text{L}/\text{min}/\text{mg}$ )	<8 / <17 / <5	<10 / <18 / <8	<20 / 41 / 23			
Hhep, Rheps, DHeaps $Cl_{\text{int}}$ ( $\mu\text{L}/\text{min}/10^6$ cells)	<8 / 8 / N.D.	15 / <5 / N. D.	7 / <5 / N.D.			
hPPB, rPPB, dPPB (Fu)	0.0016, 0.0221, 0.0055	0.0015, 0.0134, 0.0075	0.0648, 0.125, 0.231			
OATP1B1 (transfected/wild type)	N.D.	N.D.	2.05			
OATP1B3 (transfected/wild type)	N.D.	N.D.	2.13			
OATP2B1 (transfected/wild type)	N.D.	N.D.	1.83			
<b>Nav pharmacology<sup>b</sup></b>						
hNav1.1 $IC_{50}$ (nM)	8750	677	>10000			
hNav1.2 $IC_{50}$ (nM)	398	119	2044			
hNav1.3 $IC_{50}$ (nM)	>10000	>10000	>10000			
hNav1.4 $IC_{50}$ (nM)	>30000	>10000	>10000			
hNav1.5 $IC_{50}$ (nM)	>30000	>10000	>30000			
hNav1.6 $IC_{50}$ (nM)	1109	173	1636			
hNav1.7 $IC_{50}$ (nM)	21	15	46			
hNav1.8 $IC_{50}$ (nM)	>30000	>10000	>10000			
rNav1.7 $IC_{50}$ (nM)	5450	153	3140			
dNav1.7 $IC_{50}$ (nM)	132	16	263			
<b>in vivo PK</b>						
	Rat	Dog	Rat	Dog	Rat	Dog
IV dose (mg/kg)	1	0.1	1	0.1	1	0.1
$Cl_p$ (mL/min/kg)	40.3	2.0	6.0	2.7	>70	15
$Cl_u$ (mL/min/kg)	1824	364	448	360	>560	65

V <sub>ss</sub> (L/kg)	11.0	0.5	1.3	0.2	29.7	0.9
T <sub>1/2</sub> (h)	6.6	4.6	4.4	4.0	2.2	1.1
Oral dose (mg/kg)	3	3	3	3	3	N.D.
T <sub>max</sub> (h)	1.5	1.5	2.0	0.9	0.3	
C <sub>max</sub> (ng/mL)	73.2	2890	541	998	92.7	
F (%)	16	54	27	35	68	

<sup>a</sup>N.D. = not determined. <sup>b</sup>V<sub>half</sub> inactivation protocols using PatchXpress™ platform.<sup>14</sup>

The data from the human microdose study are summarized in Table 9 and Figure 5. Compound **36** was ruled out based on its short plasma half-life as the peak to trough ratios, based on twice-daily administration, would have required a high therapeutic index. Compounds **30** and **34** exhibited half-life values that would support twice-daily oral administration. However, on the basis of superior Na<sub>v</sub>1.7 potency and a PBPK modelling prediction suggesting the clinical target concentration of 3x IC<sub>50</sub> unbound plasma concentration at trough would be obtained at a lower dose, it was decided to progress compound **34** to further clinical trials. It was subsequently shown to be safe and well-tolerated up to a single oral dose of 2400 mg, providing significant coverage of the Na<sub>v</sub>1.7 IC<sub>50</sub> (C<sub>max</sub> free plasma concentration of 226 nM providing ~20x Na<sub>v</sub>1.7 IC<sub>50</sub> at the 2400 mg dose).

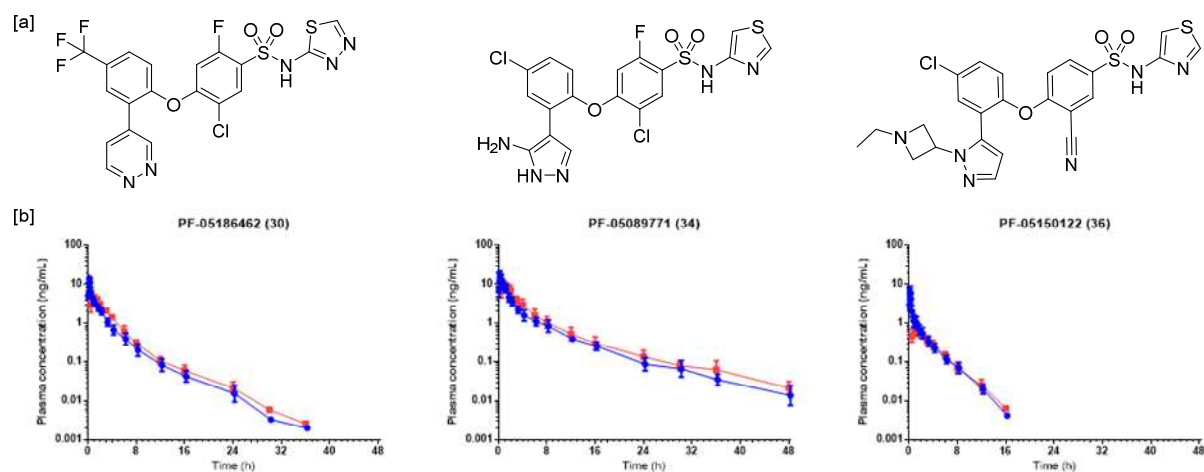


**Figure 5.** (a) Structures of **30** (PF-05186462<sup>8</sup>), **34** (PF-05089771<sup>8</sup>) and **36** (PF-05150122<sup>8</sup>). (b) Human mean plasma concentrations following 100 µg intravenous (blue) and 100 µg oral microdoses (red).

**Table 9.** Human pharmacokinetic microdose data for **30**, **34** and **36**.

Compound	<b>30</b>	<b>34</b>	<b>36</b>
IV dose (µg)	100	100	100
Cl <sub>p</sub> (mL/min/kg)	1.2	0.5	3.6
Cl <sub>u</sub> (mL/min/kg)	745	350	55
V <sub>ss</sub> (L/kg)	0.18	0.15	0.41
T <sub>1/2</sub> (h)	4.5	6.5	2.2
Oral dose (µg)	100	100	100
C <sub>max</sub> (ng/mL)	4.8	11	0.67
F (%)	101	110	52

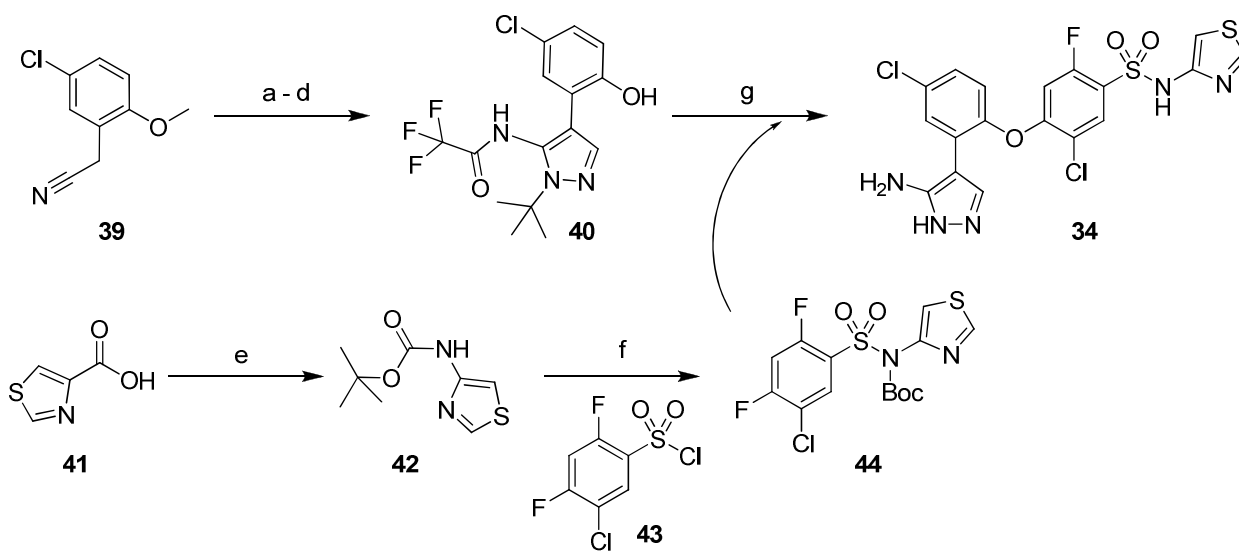
Significant in vitro and in vivo profiling of aryl sulfonamide **34** and close structural analogue **33** has been reported in an earlier manuscript.<sup>17</sup> Detailed manual electrophysiology characterization confirm **34** is a state-dependent and selective inhibitor of Na<sub>v</sub>1.7. Inhibitory effects of

compound **34** on action potentials in spinal slice electrophysiology recordings, mouse and human DRG neurons, in addition to in vivo efficacy of **33** in a mouse capsaicin-induced neurogenic flare model, further demonstrate the multiple contributions of Nav1.7 in nociceptor signaling.<sup>17</sup>

## SYNTHETIC CHEMISTRY

The key compounds **30**, **34**, **36** were prepared by S<sub>N</sub>Ar reaction, joining a heteroaryl phenol left hand side (LHS) with a suitably protected heteroaryl sulfonamide right hand side (RHS) via an ether linkage.

### Scheme 1. Synthesis of Compound **34**<sup>a</sup>



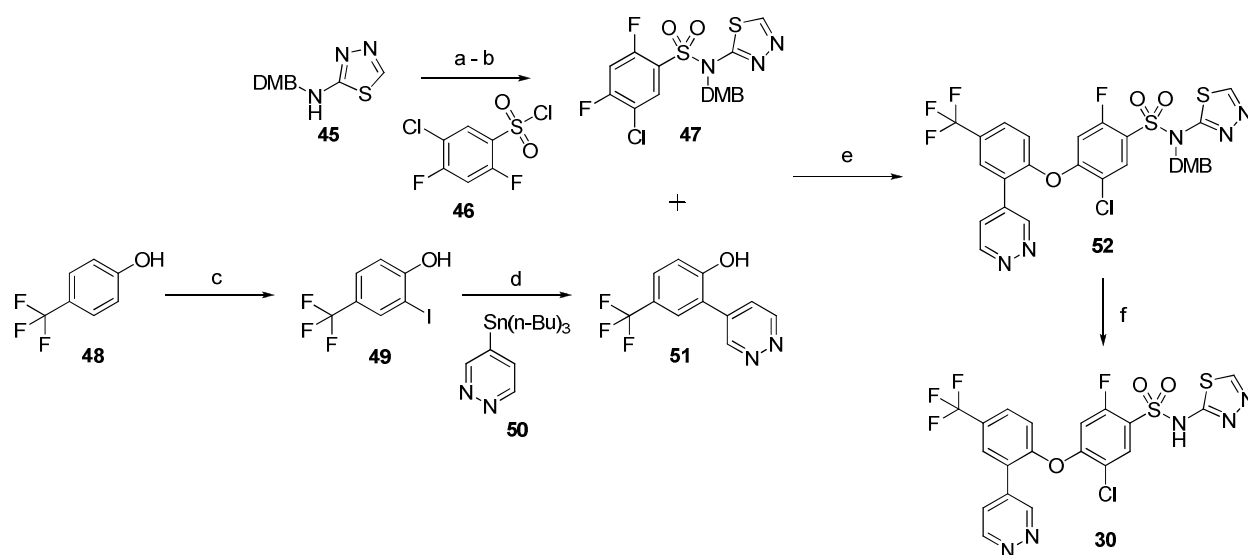
<sup>a</sup>Reagents and conditions. (a) CH<sub>3</sub>CH<sub>2</sub>OCHO, sodium, reflux, 16 h (b) (CH<sub>3</sub>)<sub>3</sub>CHNHNH<sub>2</sub>.HCl, EtOH, reflux 24 h (c) (CF<sub>3</sub>CO)<sub>2</sub>O, Et<sub>3</sub>N, CH<sub>2</sub>Cl<sub>2</sub>, 16 h (d) BBr<sub>3</sub>, CH<sub>2</sub>Cl<sub>2</sub>, 0 °C, 45 min, 66% over 4 steps (e) diphenylphosphoryl azide, t-BuOH, Et<sub>3</sub>N, reflux, 18 h, 77% (f) LiHMDS, THF, 0 °C, 30 min, 50% (g) i) NaH, DMF, ii) K<sub>2</sub>CO<sub>3</sub>, 55 °C, 3 days iii) Na<sub>2</sub>CO<sub>3</sub> (aq), CH<sub>3</sub>OH, 55 °C 16 h, iv) HCl, CH<sub>3</sub>OH, 50 °C, 16 h 12% over 4 steps.

For the synthesis of compound **34** (Scheme 1) the LHS was constructed in one pot by standard aminopyrazole ring formation utilizing 2-(5-chloro-2-methoxyphenyl)acetonitrile **39**, ethyl formate and t-butyl hydrazine hydrochloride followed by trifluoroacetate amine protection.



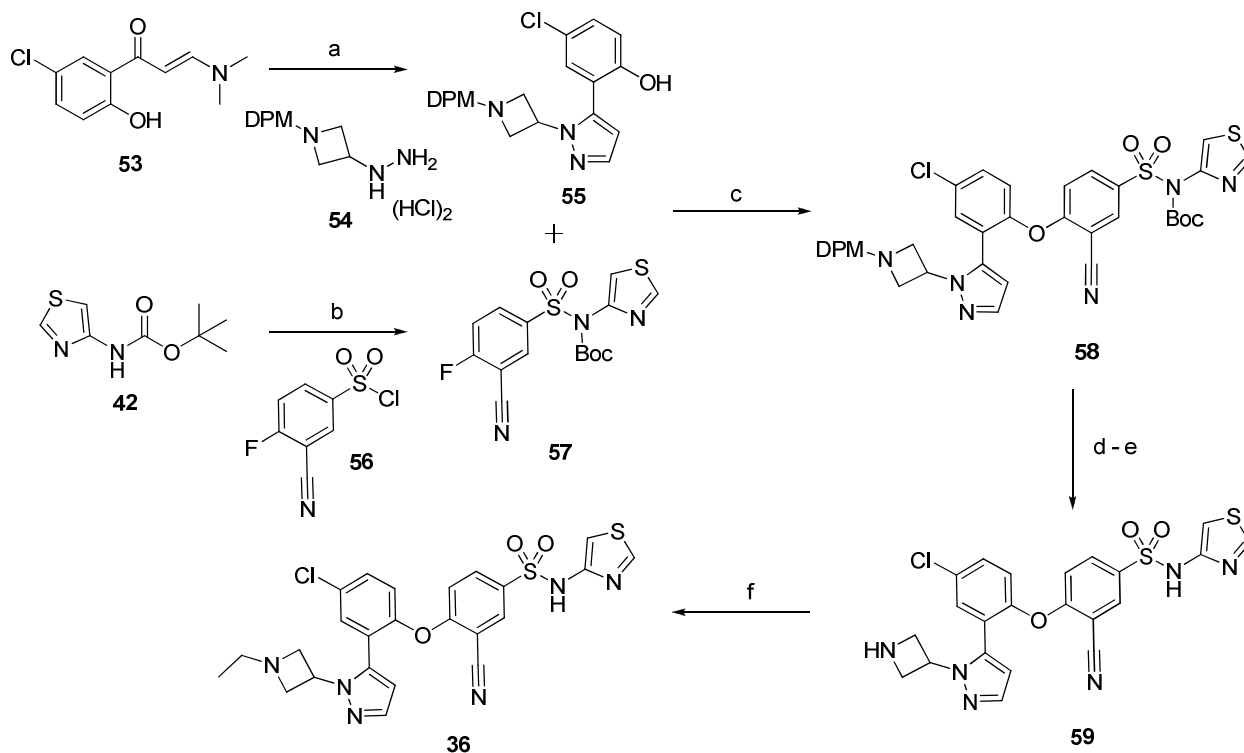
Finally boron tribromide demethylation yielded the desired phenol **40**. The protected heteroaryl sulfonamide RHS was prepared by reaction of tert-butyl thiazol-4-ylcarbamate **42** (made via Curtius rearrangement of the corresponding thiazole carboxylic acid **41**) with aryl sulfonyl chloride **43** to generate the protected RHS **44**. Base promoted  $S_NAr$  between the LHS and RHS, and subsequent protecting group removal yielded the desired final product **34**.

### Scheme 2. Synthesis of Compound **30**<sup>a</sup>



<sup>a</sup>Reagents and conditions: (a) LiHMDS, 2-Me-THF, -45 °C, 45 min.; (b) Compound **46**, -45 °C to 0 °C, 2 h, 78%; (c) Iodine, Na<sub>2</sub>CO<sub>3</sub>, THF/Water, 24 h, 41 %; (d) CH<sub>3</sub>CN, CuI, (PPh<sub>3</sub>)<sub>4</sub>, CsF, 50 °C, 2 h, 68%; (e) K<sub>2</sub>CO<sub>3</sub>, DMSO, 16 h, 67%; (f) 4M HCl / dioxane, 3 h, 82%

Synthesis of compound **30** (Scheme 2) was initiated by aryl sulfonyl chloride **46** addition to 2,4-dimethoxybenzyl (DMB) protected aminothiadiazole **45** to build the RHS for this scaffold. Construction of the LHS was achieved by iodination of 4-trifluoromethyl phenol **48** to yield compound **49** followed by copper mediated addition of 4-(tributylstannyl) pyridazine **50** to construct diaryl phenol **51**. Finally base mediated  $S_NAr$  and HCl cleavage of the DMB protecting group gave compound **30**.

Scheme 3. Synthesis of Compound **36**<sup>a</sup>

<sup>a</sup>Reagents and Conditions (a) Compounds **53** and **54** (see SI for synthesis), EtOH, 0 °C, 2 h, 42%; (b) LiHMDS, -78 °C to room temp., 16 h, 54%; (c) K<sub>2</sub>CO<sub>3</sub>, DMSO, room temp. 4 h, 24%; (d) i) Chloroethyl chloroformate, proton sponge, CH<sub>2</sub>Cl<sub>2</sub>, room temp. 3.5 h. ii) CH<sub>3</sub>OH, reflux, 4 h; (e) 4M HCl/dioxane, 2 h, 33% over 3 steps; (f) Sodium triacetoxyborohydride, CH<sub>2</sub>Cl<sub>2</sub>/CH<sub>3</sub>OH, Et<sub>3</sub>N, 0 °C, acetaldehyde, 1.5 h, 60%.

In an analogous manner the LHS of compound **36** (Scheme 3) was prepared by standard condensation of enamine **53** with diphenylmethyl (DPM) protected azetidyl-hydrazine hydrochloride **54** to generate the required phenol **55**. The RHS **57** was prepared analogously to that in Scheme 1 and subsequent  $S_NAr$  provided fully protected **58**. DPM removal via treatment with proton sponge and chloroethyl chloroformate followed by complete Boc removal with HCl gave the desired fully deprotected **59**. Finally, reductive amination with acetaldehyde gave the desired compound **36**.

## CONCLUSIONS

1  
2  
3 In summary, a series of diaryl ether aryl sulfonamides has been identified as potent and highly  
4 subtype selective inhibitors of Na<sub>v</sub>1.7. This high molecular weight, acidic chemotype  
5 represented a significant challenge in human pharmacokinetic predictions due to non-metabolic  
6 clearance pathways predominating. A human microdose study was therefore carried out on 3  
7 diverse ligands from the series (varying pK<sub>a</sub>, lipophilicity and chemical diversity) to determine  
8 basic PK parameters leading to the nomination of **34** as a clinical candidate. Furthermore, this  
9 represents the first potent and selective molecule which binds to the domain IV voltage sensor  
10 region of the sodium channel to progress into the clinic. The development of selective agents  
11 such as **34** offers new potential therapeutic modalities for acute and chronic pain, which remain a  
12 high medical need.  
13  
14  
15  
16  
17  
18  
19  
20  
21  
22  
23  
24  
25  
26  
27  
28

## 29 EXPERIMENTAL SECTION

30  
31 The synthesis of the lead compounds **30**, **34**, **36** are described below. Detailed experimental  
32 procedures for the synthesis of all other compounds, their intermediates, and characterization  
33 data are provided in the supporting information.  
34  
35  
36  
37

38 **Materials and Methods.** Unless otherwise noted, all materials were obtained from  
39 commercial suppliers and used without further purification. <sup>1</sup>H Nuclear magnetic resonance  
40 (NMR) spectra were in all cases consistent with the proposed structures. Characteristic chemical  
41 shifts (δ) are given in parts-per-million (ppm) (δ relative to residual solvent peak) using  
42 conventional abbreviations for designation of major peaks: *e.g.* s, singlet; d, doublet; t, triplet; m,  
43 multiplet; br, broad. The mass spectra (*m/z*) were recorded electrospray ionization (ESI). The  
44 following abbreviations have been used for common solvents: CDCl<sub>3</sub>, deuteriochloroform; d<sub>6</sub>-  
45 DMSO, deuterodimethylsulfoxide; CD<sub>3</sub>OD, deuteromethanol. All solvents were reagent grade  
46  
47  
48  
49  
50  
51  
52  
53  
54  
55  
56  
57  
58  
59  
60

1  
2  
3 and, when necessary, were purified and dried by standard methods. Concentration of solutions  
4  
5 after reactions and extractions involved the use of a rotary evaporator operating at a reduced  
6  
7 pressure of ca. 20 Torr. Anhydrous solvents were obtained from commercial sources and used as  
8  
9 supplied. Organic solvents were dried over anhydrous magnesium sulfate or anhydrous sodium  
10  
11 sulfate. All final compounds had a high performance liquid chromatography (HPLC) purity of  
12  
13 95% or greater using one of the methods described in the supporting information.  
14  
15

16  
17 **5-Chloro-2-fluoro-4-[2-pyridazin-4-yl-4-(trifluoromethyl)phenoxy]-N-1,3,4-thiadiazol-2-**  
18  
19 **ylbenzenesulfonamide (30).** To a stirred solution of 5-chloro-N-(2,4-dimethoxybenzyl)-2-  
20  
21 fluoro-4-[2-pyridazin-4-yl-4-(trifluoromethyl)phenoxy]-N-1,3,4-thiadiazol-2-  
22  
23 ylbenzenesulfonamide (**52**) (28.1 g, 41.2 mmol) in 1,4-dioxane (250 mL) at room temperature  
24  
25 was added a 4M solution of HCl in 1,4-dioxane (300 mL) dropwise over 30 minutes. The  
26  
27 resulting suspension was left to stir at room temperature for 3 hours before concentration in  
28  
29 vacuo. The residue was azeotroped with diethyl ether (3 x 300 mL) followed by a diethyl ether  
30  
31 trituration (200 mL) to provide crude material as a fawn colored solid. This material was  
32  
33 suspended in methanol (200 mL) and filtered through Celite, washed with methanol (400 mL)  
34  
35 and the resulting filtrate concentrated in vacuo to give a sand colored solid. This material was  
36  
37 suspended in water (100 mL) and treated with concentrated ammonium hydroxide (60 mL)  
38  
39 portion wise until pH 9-10 was achieved. The resulting solution was washed with diethyl ether  
40  
41 (3 x 75 mL) and the aqueous layer acidified to pH=5 with citric acid. The mixture was then  
42  
43 extracted with ethyl acetate (3 x 200 mL) and brine (100 mL) added to aid separation. The  
44  
45 combined organic layers were washed with water (200 mL), dried over MgSO<sub>4</sub> and concentrated  
46  
47 in vacuo to approximately 100 mL whereby a precipitate was observed. This mixture was  
48  
49 allowed to stand for 18 hours and the resulting solid filtered and washed with cold ethyl acetate  
50  
51  
52  
53  
54  
55  
56  
57  
58  
59  
60

(10 mL) and dried in vacuo at 60 °C to provide the title compound as a sand colored crystalline solid (17.5 g, 80%). <sup>1</sup>H NMR (400 MHz, DMSO-*d*<sub>6</sub>) δ ppm 7.31 (d, *J*=8.60 Hz, 1 H) 7.51 (d, *J*=10.55 Hz, 1 H) 7.87 (dd, *J*=8.99, 2.34 Hz, 1 H) 7.92 - 8.03 (m, 2 H) 8.12 (d, *J*=2.34 Hz, 1 H) 8.83 (s, 1 H) 9.33 (dd, *J*=5.27, 1.37 Hz, 1 H) 9.52 (dd, *J*=2.54, 1.37 Hz, 1 H). HPLC (12min) *t*<sub>R</sub>= 8.35 min, HPLC purity >98%. LCMS (APCI) *m/z* 532 [M+H]<sup>+</sup> HRMS (EI) *m/z*: [M+H]<sup>+</sup> Calcd for C<sub>19</sub>H<sub>11</sub>ClF<sub>4</sub>N<sub>5</sub>O<sub>3</sub>S<sub>2</sub> 531.9928, found 531.9919.

**4-[2-(5-Amino-1H-pyrazol-4-yl)-4-chlorophenoxy]-5-chloro-2-fluoro-N-1, 3-thiazol-4-ylbenzenesulfonamide (34).** To a suspension of sodium hydride (29 mg, 1.2 mmol) in dimethylformamide (1 mL) was added N-(1-tert-butyl-4-(5-chloro-2-hydroxyphenyl)-1H-pyrazol-5-yl)-2,2,2-trifluoroacetamide (**40**) (239 mg, 0.661 mmol) and stirred for 30 minutes. To this was added tert-butyl 5-chloro-2, 4-difluorophenylsulfonyl (thiazol-4-yl) carbamate (**44**) (206 mg, 0.501 mmol) and the reaction stirred for 24 hours. Potassium carbonate (40 mg, 0.3 mmol) was added and the reaction heated at 55 °C for 3 days. The reaction was cooled, diluted with ethyl acetate (10 mL) and the organic extract washed with water (10 mL) and saturated aqueous sodium chloride solution (10 mL), dried over magnesium sulfate, filtered and concentrated in vacuo. Purification by automated flash column chromatography eluting with ethyl acetate:hexanes (gradient 0:1 to 1:0) afforded intermediate protected product. This residue was dissolved in methanol (1 mL) and sodium carbonate solution (2 M aqueous, 0.08 mL, 0.2 mmol) and water (0.2 mL) added. The reaction was stirred at room temperature for 6 hours and then heated at 55 °C for 16 hours before concentrating in vacuo and purification by flash chromatography eluting with methanol:dichloromethane (gradient 0:1 to 1:9). The resulting purified material was dissolved in methanol (saturated in gaseous hydrogen chloride) and heated at 50 °C for 16 hours. Purification by preparative HPLC afforded the title compound HCl salt as

1  
2  
3 a white solid (31 mg, 12%). <sup>1</sup>H NMR - HCl salt (600 MHz, DMSO-d<sub>6</sub>) δ ppm 6.98 (d, *J*=11.15  
4 Hz, 1 H) 7.10 (d, *J*=1.17 Hz, 1 H) 7.22 (d, *J*=8.80 Hz, 1 H) 7.47 (dd, *J*=8.51, 2.05 Hz, 1 H) 7.73  
5 (br. s., 1 H) 7.90 (d, *J*=7.04 Hz, 1 H) 7.94 (s, 1 H) 8.92 (d, *J*=1.17 Hz, 1 H) <sup>1</sup>H NMR - Free  
6 base: (600 MHz, DMSO-d<sub>6</sub>) δ ppm 4.85 (br. s., 2 H) 6.72 (d, *J*=10.56 Hz, 1 H) 7.07 (d, *J*=1.17  
7 Hz, 1 H) 7.21 (d, *J*=8.80 Hz, 1 H) 7.28 - 7.34 (m, 1 H) 7.42 (br. s., 1 H) 7.68 (br. s., 1 H) 7.89 (d,  
8 *J*=7.04 Hz, 1 H) 8.90 (d, *J*=1.76 Hz, 1 H) 11.37 (br. s., 1 H) 11.72 (br. s., 1 H), HPLC (12min)  
9 *t<sub>R</sub>*= 7.66 min, HPLC purity >98%. LRMS (ESI) *m/z* 501 [M+H]<sup>+</sup>; HRMS (EI) *m/z*: [M+H]<sup>+</sup>  
10  
11  
12  
13  
14  
15  
16  
17  
18  
19  
20 Calcd for C<sub>18</sub>H<sub>13</sub>Cl<sub>2</sub>FN<sub>5</sub>O<sub>3</sub>S<sub>2</sub> 499.9821, found 499.9816.

21  
22 **4-{4-Chloro-2-[1-(1-ethylazetidin-3-yl)-1H-pyrazol-5-yl]phenoxy}-3-cyano-N-1,3-thiazol-**  
23 **4-ylbenzenesulfonamide (36).** To a suspension of 4-[2-(1-azetidin-3-yl-1H-pyrazol-5-yl)-4-  
24 chlorophenoxy]-3-cyano-N-1,3-thiazol-4-ylbenzenesulfonamide, (**59**) (500 mg, 0.797 mmol) in  
25 methanol (4 mL) and dichloromethane (4 mL) was added triethylamine (161 mg, 1.59 mmol) and  
26 the reaction cooled to 0 °C in an ice/water bath. To the suspension was added sodium  
27 triacetoxyborohydride (422 mg, 1.99 mmol) and the reaction was then stirred at 0 °C for 10  
28 minutes. Acetaldehyde (105 mg, 2.39 mmol) was added dropwise and the reaction stirred at 0 °C  
29 for 1.5 hours. The solvent was removed *in vacuo* to give an orange oil which was partitioned  
30 between dichloromethane (25 mL) and water (25 mL). The organic layer was separated and the  
31 aqueous layer was extracted with dichloromethane (2 x 20 mL). The combined organic layers  
32 were washed with saturated aqueous sodium chloride solution (20 mL) and filtered through a  
33 phase separation cartridge. The solvent was removed *in vacuo* and the resulting solid was  
34 triturated in hot ethyl acetate (10 mL), allowed to cool to room temperature and then filtered to  
35 provide the title compound as a white solid (260 mg, 60%). <sup>1</sup>H NMR (400 MHz, DMSO-*d*<sub>6</sub>) δ  
36 ppm 1.04 - 1.13 (m, 3 H) 3.24 (q, *J*=6.64 Hz, 2 H) 4.16 (br. s., 2 H) 4.42 (br. s., 2 H) 5.11 (br. s.,  
37  
38  
39  
40  
41  
42  
43  
44  
45  
46  
47  
48  
49  
50  
51  
52  
53  
54  
55  
56  
57  
58  
59  
60

1  
2  
3 1 H) 6.28 (d,  $J=1.95$  Hz, 1 H) 6.97 (d,  $J=8.99$  Hz, 1 H) 7.09 (d,  $J=1.95$  Hz, 1 H) 7.51 (d,  $J=8.60$   
4 Hz, 1 H) 7.61 (d,  $J=1.17$  Hz, 1 H) 7.68 - 7.75 (m, 2 H) 7.87 (dd,  $J=8.99, 2.34$  Hz, 1 H) 8.09 -  
5  
6 8.15 (m, 1 H) 8.90 (d,  $J=2.34$  Hz, 1 H) 10.94 (br. s., 1 H). HPLC (12min)  $t_R= 7.57$  min, HPLC  
7  
8 purity >98%. LCMS (ESI)  $m/z$  541  $[M+H]^+$ ; HRMS (EI)  $m/z$ :  $[M+H]^+$  Calcd for  
9  
10  $C_{24}H_{22}ClN_6O_3S_2$ , 541.0883 found 541.0935.  
11  
12

13  
14  
15 **N-[1-*tert*-Butyl-4-(5-chloro-2-hydroxyphenyl)-1H-pyrazol-5-yl]-2,2,2-trifluoroacetamide**

16  
17 **(40)**. To a solution of (5-chloro-2-methoxy-phenyl)acetonitrile (**39**) (2.154 g, 11.86 mmol) in  
18 ethyl formate (20 mL) was added sodium (605 mg, 26.3 mmol). The reaction was heated at a  
19 gentle reflux for 16 hours. After cooling to room temperature, water and dichloromethane were  
20 added and the solution adjusted to pH 3 with hydrochloric acid (6 M aqueous solution). The  
21 layers were separated and the aqueous layer extracted with dichloromethane (2 x 50 mL). The  
22 combined organics were washed with saturated aqueous sodium chloride solution, dried over  
23 magnesium sulfate, filtered and evaporated *in vacuo*. Purification by flash column  
24 chromatography eluting with ethyl acetate: hexanes (gradient 0:1 to 1:1, by volume) gave a white  
25 solid which was dissolved in ethanol (50 mL), *tert*-butylhydrazine hydrochloride (1.77 g, 14.2  
26 mmol) added and solution heated to reflux for 24 hours. The reaction was cooled and evaporated  
27 *in vacuo* to give brown oil. This oil was dissolved in dichloromethane (50 mL) and  
28 triethylamine (4.2 mL, 30 mmol) and trifluoroacetic anhydride (4.2 mL, 30 mmol) were added.  
29 After stirring for 16 hours, the reaction was washed with potassium hydrogen sulfate (1 N  
30 aqueous solution), sodium bicarbonate (1 N aqueous solution) and saturated aqueous sodium  
31 chloride solution. The organic layer was separated, dried over magnesium sulfate, filtered and  
32 concentrated *in vacuo* to give brown oil. This oil was dissolved in dichloromethane (20 mL) and  
33 cooled over an ice water bath before the addition of boron tribromide (1 M in dichloromethane,  
34  
35  
36  
37  
38  
39  
40  
41  
42  
43  
44  
45  
46  
47  
48  
49  
50  
51  
52  
53  
54  
55  
56  
57  
58  
59  
60

1  
2  
3 22 mL, 22 mmol). After stirring for 45 minutes the reaction was added to ice water. The layers  
4  
5 were separated and the aqueous layer washed with dichloromethane (2 x 20 mL). The combined  
6  
7 organics were dried over magnesium sulfate, filtered and concentrated *in vacuo* to give brown  
8  
9 oil. Purification by flash column chromatography eluting with ethyl acetate: hexane (gradient  
10  
11 0:1 to 1:0, by volume) to afford the title compound as a brown oil that solidified to a tan solid  
12  
13 upon standing (2.82 g, 66%). <sup>1</sup>H NMR (400 MHz, DMSO-*d*<sub>6</sub>) δ ppm 1.56 (s, 9 H) 6.90 (d,  
14  
15 *J*=8.58 Hz, 1 H) 7.08 - 7.15 (m, 1 H) 7.17 (d, *J*=2.73 Hz, 1 H) 7.76 (s, 1 H) 9.91 (s, 1 H) 11.38  
16  
17 (s, 1 H). HPLC (6 min), *t*<sub>R</sub> = 3.0 min, HPLC purity >95%. LCMS (ESI) *m/z* 362.4 [M+H]<sup>+</sup>.  
18  
19

20  
21  
22 **Thiazole-4-yl-carbamic acid *tert*-butyl ester (42).** Thiazole-4-carboxylic acid (41) (10 g,  
23  
24 77.4 mmol) was slurried in *tert*-butyl alcohol (500 mL). Triethylamine (11.9 mL, 85.2 mmol)  
25  
26 and diphenylphosphonic azide (18.4 mL, 85.2 mmol) were added and the reaction was heated at  
27  
28 reflux for 18 hours. The reaction was evaporated to a residue. The residue was dissolved in ethyl  
29  
30 acetate (250 mL) and washed with water (100 mL), 5% citric acid (aqueous, 100 mL), water  
31  
32 (100 mL), saturated aqueous sodium bicarbonate (100 mL) and brine (100 mL). The organic  
33  
34 phase was dried over magnesium sulfate and evaporated to a brown solid. The solid was purified  
35  
36 by silica gel chromatography in 5%-40% ethyl acetate / hexane gradient elution to afford the title  
37  
38 compound as a colorless solid (12.8 g, 77.4%). <sup>1</sup>H NMR (400 MHz, DMSO-*d*<sub>6</sub>) δ ppm 1.45 (s, 9  
39  
40 H) 7.21 (br. s., 1 H) 8.87 (d, *J*=2.34 Hz, 1 H) 10.17 (br. s., 1 H). HPLC (12 min), *t*<sub>R</sub> = 8.09 min,  
41  
42 HPLC purity >95%. LCMS (ESI) *m/z* 201 [M+H]<sup>+</sup>.  
43  
44  
45  
46  
47

48  
49 ***tert*-Butyl ((5-chloro-2, 4-difluorophenyl) sulfonyl) (thiazol-4-yl) carbamate (44).** A THF  
50  
51 (2 mL) solution of *tert*-butyl thiazol-4-ylcarbamate (42) (195 mg, 0.97 mmol) was treated with a  
52  
53 solution of 1M LiHMDS in THF (972 μL, 0.97 mmol) at 0 °C and stirred for 30 minutes. Then,  
54  
55 5-chloro-2, 4-difluorobenzenesulfonyl chloride (43) (200 mg, 0.810 mmol) was added at 0 °C.  
56  
57  
58  
59  
60



1  
2  
3 The mixture was allowed to warm to room temperature and stirred overnight. The mixture was  
4 treated with water (6 mL) and stirred for 1 hour. The resulting precipitate was filtered and  
5 purified by column chromatography eluting with a gradient of 100% heptanes to 50% EtOAc /  
6 heptanes to afford the title compound as a colorless solid (166 mg, 50%). <sup>1</sup>H NMR (400 MHz,  
7 CDCl<sub>3</sub>) δ ppm 1.39 (s, 9 H) 7.10 (t, *J*=8.79 Hz, 1 H) 7.54 (d, *J*=2.15 Hz, 1 H) 8.25 (t, *J*=7.52 Hz,  
8 1 H) 8.80 (d, *J*=2.15 Hz, 1 H). HPLC (6 min), *t*<sub>R</sub> = 2.9 min, HPLC purity >95%. LCMS (ESI)  
9 *m/z* 411 [M+H]<sup>+</sup>.

10  
11  
12  
13  
14  
15  
16  
17  
18  
19  
20 **5-Chloro-N-(2,4-dimethoxybenzyl)-2,4-difluoro-N-1,3,4-thiadiazol-2-**  
21  
22 **ylbenzenesulfonamide (47).** To a suspension of the N-(2,4-dimethoxybenzyl)-1,3,4-thiadiazol-  
23 2-amine (45) (27.7 g, 110 mmol) in 2-methyl-THF (225 mL) at -45 °C was added dropwise a  
24 solution of LiHMDS (1M in THF, 121mL, 121 mmol) maintaining temp between -40 to -45 °C.  
25 After addition the heterogeneous mixture allowed to stir at -45 °C for 45 minutes. To the  
26 resultant suspension at -45 °C was added a 2-methyl-THF solution (45 mL) of 5-chloro-2,4-  
27 difluorobenzenesulfonyl chloride (46) (27.2 g, 110 mmol) at such a rate as to maintain the temp  
28 between -45 °C to -40 °C. After addition the resultant orange solution was allowed to warm to 0  
29 °C over 2 hours. The reaction was quenched with a saturated aqueous ammonium chloride  
30 solution and extracted with EtOAc. The organic layers were washed with water and brine, dried  
31 over MgSO<sub>4</sub>, before concentration in vacuo to give an oil. Purification was accomplished by  
32 flash chromatography eluting with 30-50% EtOAc/heptanes to provide the title compound as a  
33 pale yellow solid (39.9 g, 78%). <sup>1</sup>H NMR (500 MHz, CDCl<sub>3</sub>) δ ppm 3.73 (s, 3 H) 3.78 (s, 3 H)  
34 5.35 (s, 2 H) 6.29 (d, *J*=2.44 Hz, 1 H) 6.38 (dd, *J*=8.42, 2.32 Hz, 1 H) 6.98 (t, *J*=8.78 Hz, 1 H)  
35 7.29 (d, *J*=2.68 Hz, 1 H) 7.84 (t, *J*=7.44 Hz, 1 H) 8.87 (s, 1 H). HPLC (5 min), *t*<sub>R</sub> = 3.59 min,  
36 HPLC purity >95%. LCMS (ESI) *m/z*, 462 [M+H]<sup>+</sup>.  
37  
38  
39  
40  
41  
42  
43  
44  
45  
46  
47  
48  
49  
50  
51  
52  
53  
54  
55  
56  
57  
58  
59  
60

1  
2  
3       **2-Iodo-4-(trifluoromethyl) phenol (49).** A mixture of iodine (23.2 g, 91.6 mmol), and  
4 sodium carbonate (7.7 g, 91.6 mmol,) was added to a solution of 4-(trifluoromethyl) phenol (**48**)  
5 (13.5 g, 83.3 mmol,) in THF (90 mL) and water (90 mL), then the reaction was allowed to stir at  
6 room temperature for 18 hours. Sufficient thiourea (5% solution) was added to remove the  
7 excess iodine, as indicated by the color change of the reaction from deep violet to brown. The  
8 reaction mixture was then extracted with diethyl ether. The organic phase was dried over  
9 MgSO<sub>4</sub>, concentrated in vacuo to give brown oil. This was purified by silica gel chromatography  
10 (E<sub>2</sub>O:Hexane = 1:10) followed by trituration with Et<sub>2</sub>O/hexane to provide the title compound as a  
11 tan solid (9.84 g, 41%). <sup>1</sup>H NMR (400 MHz, CDCl<sub>3</sub>) δ ppm 6.07 (s, 1 H) 7.94 (s, 2 H). HPLC (2  
12 min), t<sub>R</sub> = 1.53 min, HPLC purity >95%. LCMS (ESI) *m/z* 288.1 [M+H]<sup>+</sup>.  
13  
14  
15  
16  
17  
18  
19  
20  
21  
22  
23  
24  
25  
26

27       **2-Pyridazin-4-yl-4-(trifluoromethyl)phenol (51).** To an argon flushed flask containing a  
28 solution of 4-(tributylstannyl)pyridazine (**50**) (5.0 g, 13.5 mmol) in acetonitrile (20 mL) was  
29 added 2-iodo-4-(trifluoromethyl)phenol, (**49**) (3.9 g, 13.5 mmol) in acetonitrile (30 mL). Copper  
30 iodide (500 mg, 2.63 mmol) was added followed by Pd(PPh<sub>3</sub>)<sub>4</sub> (750 mg, 0.65 mmol) and cesium  
31 fluoride (4.1 g, 27 mmol). The mixture was heated to 50 °C for 2 hours and allowed to cool  
32 before concentrating in vacuo. The residue was partitioned between dichloromethane (50 mL)  
33 and aqueous 2M HCl (100 mL)/water (20 mL). The organic layer was re-extracted with aqueous  
34 2M HCl (15 mL) and the combined aqueous extracts were neutralized by adding solid NaHCO<sub>3</sub>  
35 slowly. The mixture was then extracted with EtOAc (100 mL), dried over Na<sub>2</sub>SO<sub>4</sub> and  
36 concentrated in vacuo to provide the title compound as a solid (2.2 g, 68%). <sup>1</sup>H NMR (400 MHz,  
37 DMSO-*d*<sub>6</sub>) δ ppm 7.19 (d, *J*=8.40 Hz, 1 H) 7.68 (dd, *J*=8.69, 2.05 Hz, 1 H) 7.83 (d, *J*=1.76 Hz, 1  
38 H) 7.95 (d, *J*=3.51 Hz, 1 H) 9.29 (br. s., 1 H) 9.52 (br. s., 1 H) 11.11 (s, 1 H). LCMS (ESI) *m/z*  
39 241 [M+H]<sup>+</sup>.  
40  
41  
42  
43  
44  
45  
46  
47  
48  
49  
50  
51  
52  
53  
54  
55  
56  
57  
58  
59  
60

1  
2  
3  
4  
5  
6  
7  
8  
9  
10  
11  
12  
13  
14  
15  
16  
17  
18  
19  
20  
21  
22  
23  
24  
25  
26  
27  
28  
29  
30  
31  
32  
33  
34  
35  
36  
37  
38  
39  
40  
41  
42  
43  
44  
45  
46  
47  
48  
49  
50  
51  
52  
53  
54  
55  
56  
57  
58  
59  
60

**5-Chloro-N-(2,4-dimethoxybenzyl)-2-fluoro-4-[2-pyridazin-4-yl-4-(trifluoromethyl)phenoxy]-N-1,3,4-thiadiazol-2-ylbenzenesulfonamide (52).** A stirred solution of the 2-pyridazin-4-yl-4-(trifluoromethyl) phenol (**51**) (890 mg, 3.7 mmol) in DMSO (10 mL) was treated with potassium carbonate (563 mg, 4.08 mmol) and the mixture stirred for 1 minute. Solid 5-chloro-N-(2,4-dimethoxybenzyl)-2,4-difluoro-N-1,3,4-thiadiazol-2-ylbenzenesulfonamide (**47**) (1.71 g, 3.7 mmol) was then added portion-wise and the reaction mixture stirred at room temperature for 18 hours. The reaction mixture was poured onto aqueous 1M NaOH (120 mL) and the resulting precipitate extracted with EtOAc (3 x 100 mL). The combined organic extracts were washed with water and dried over MgSO<sub>4</sub> to give a foam. Purification by flash column chromatography, eluting with a gradient of 50% EtOAc/heptane to 100% EtOAc gave the title compound as a foam (1.69 g, 67%). <sup>1</sup>H NMR (400 MHz, CDCl<sub>3</sub>) δ ppm 3.71 (s, 3 H) 3.75 (s, 3 H) 5.33 (s, 2 H) 6.27 (d, *J*=2.15 Hz, 1 H) 6.36 (dd, *J*=8.40, 2.34 Hz, 1 H) 6.62 (d, *J*=9.76 Hz, 1 H) 7.07 (d, *J*=8.40 Hz, 1 H) 7.26 - 7.33 (m, 1 H partially obscured by chloroform) 7.71 (dd, *J*=5.27, 2.34 Hz, 1 H) 7.77 - 7.84 (m, 2 H) 7.87 (d, *J*=6.83 Hz, 1 H) 8.85 (s, 1 H) 9.31 (d, *J*=5.27 Hz, 1 H) 9.46 (s, 1 H). HPLC (2 min), *t*<sub>R</sub> = 1.79 min, HPLC purity >95%. LCMS (ESI) *m/z* 682 [M+H]<sup>+</sup>.

**4-Chloro-2-{1-[1-(diphenylmethyl)azetid-3-yl]-1H-pyrazol-5-yl} phenol (55).** 1-(diphenylmethyl)-3-hydrazinoazetid-3-yl dihydrochloride (**54**) (1.00 g, 3.06 mmol) was added to an ice cold, stirred suspension of (2*E*)-1-(5-chloro-2-hydroxyphenyl)-3-(dimethylamino)prop-2-en-1-one (**53**) (700 mg, 3.1 mmol) in ethanol (5 mL) and acetic acid (5 mL), stirred at 0 °C for 2 hours then allowed to warm to room temperature over 2 hours. The solvents were removed in vacuo and the residue partitioned between ethyl acetate (80 mL) and saturated aqueous sodium hydrogen carbonate solution (50 mL). The organic layer was separated and dried over sodium

1  
2  
3 sulfate, filtered and the solvents removed in vacuo to give a yellow gum. This was dissolved in  
4 warm methyl-*t*-butyl ether (20 mL) and allowed to crystallize to provide the title compound as a  
5 pale yellow powder (541 mg, 42%). <sup>1</sup>H NMR (400 MHz, CDCl<sub>3</sub>) δ ppm 3.63 (dd, *J*=7.52, 1.85  
6 Hz, 4 H) 4.61 (s, 1 H) 4.86 (quin, *J*=7.47 Hz, 1 H) 6.33 (d, *J*=1.76 Hz, 1 H) 6.88 (d, *J*=8.79 Hz, 1  
7 H) 7.08 (d, *J*=2.54 Hz, 1 H) 7.15 - 7.22 (m, 2 H) 7.23 - 7.35 (m, 5 H) 7.39 - 7.49 (m, 5 H) 7.70  
8 (d, *J*=1.76 Hz, 1 H). HPLC (6 min), *t*<sub>R</sub> = 1.27 min, HPLC purity >95%. LCMS (ESI) *m/z* 416  
9 [M+H]<sup>+</sup>.

10  
11  
12  
13  
14  
15  
16  
17  
18  
19  
20 ***tert*-Butyl ((3-cyano-4-fluorophenyl)sulfonyl)(thiazol-4-yl)carbamate (57).** To a stirred  
21 solution of *tert*-butyl 1,3-thiazol-4-ylcarbamate (**42**) (0.500 g, 2.497 mmol) in tetrahydrofuran  
22 (10 mL) was added lithium 1,1,1,3,3,3-hexamethyldisilazan-2-ide (1.0 M solution in  
23 tetrahydrofuran, 2.50 mL, 2.5 mmol) at 0 °C under nitrogen. After stirring for 1 hour at 0 °C the  
24 reaction mixture was cooled to -78 °C and 3-cyano-4-fluorobenzenesulfonyl chloride (**56**) (0.453  
25 g, 2.063 mmol) in tetrahydrofuran (5.0 mL) was added. The mixture was warmed to room  
26 temperature for 16 hours. Saturated aqueous ammonium chloride solution (20 mL) was added  
27 and the aqueous layer was extracted with ethyl acetate (3 x 20 mL). Combined organic layers  
28 were dried over sodium sulfate and concentrated *in vacuo*. This crude residue was purified by  
29 flash chromatography eluting with ethyl acetate:dichloromethane (gradient 0:1 to 3:7) to afford  
30 the title compound as a white solid (426 mg, 54%). <sup>1</sup>H NMR (400 MHz, DMSO-*d*<sub>6</sub>) δ ppm 1.26  
31 (s, 9 H) 7.91 (t, *J*=8.99 Hz, 1 H) 8.18 (d, *J*=2.34 Hz, 1 H) 8.45 (ddd, *J*=9.08, 4.79, 2.54 Hz, 1 H)  
32 8.59 (dd, *J*=5.86, 2.34 Hz, 1 H) 9.18 (d, *J*=2.34 Hz, 1 H). LCMS (ESI) *m/z* 384 [M+H]<sup>+</sup>.

33  
34  
35  
36  
37  
38  
39  
40  
41  
42  
43  
44  
45  
46  
47  
48  
49  
50  
51 ***tert*-Butyl{[4-(4-chloro-2-{1-[1-(diphenylmethyl)azetid-3-yl]-1*H*-pyrazol-5-yl}phenoxy)-**  
52 **3-cyanophenyl]sulfonyl}1,3-thiazol-4-ylcarbamate (58).** 4-chloro-2-{1-[1-  
53 (diphenylmethyl)azetid-3-yl]-1*H*-pyrazol-5-yl}phenol, (**55**) (75 mg, 0.18 mmol), *tert*-butyl [(3-  
54  
55  
56  
57  
58  
59  
60

1  
2  
3  
4  
5  
6  
7  
8  
9  
10  
11  
12  
13  
14  
15  
16  
17  
18  
19  
20  
21  
22  
23  
24  
25  
26  
27  
28  
29  
30  
31  
32  
33  
34  
35  
36  
37  
38  
39  
40  
41  
42  
43  
44  
45  
46  
47  
48  
49  
50  
51  
52  
53  
54  
55  
56  
57  
58  
59  
60

cyano-4-fluorophenyl)sulfonyl]1,3-thiazol-4-ylcarbamate (**57**) (69 mg, 0.18 mmol), potassium carbonate (62 mg, 0.45 mmol) and dimethyl sulfoxide (4 mL) were combined and stirred at room temperature under nitrogen for 4 hours. Saturated aqueous ammonium chloride solution (20 mL) was added and the mixture extracted with ethyl acetate (20 mL). The organic layer was separated and back-washed with saturated aqueous sodium chloride solution (2 x 20 mL). The organic layer was separated, dried over sodium sulfate, filtered and evaporated to give an oil. The oil was purified by flash chromatography, eluting with a gradient from dichloromethane to dichloromethane: methanol (98:2) to provide the title compound as a glassy solid (33 mg, 24%). <sup>1</sup>H NMR (400 MHz, CDCl<sub>3</sub>) δ ppm 1.32 (s, 9 H) 3.55 - 3.63 (m, 2 H) 3.64 - 3.71 (m, 2 H) 4.57 (s, 1 H) 4.92 (quin, *J*=7.22 Hz, 1 H) 6.22 (d, *J*=1.76 Hz, 1 H) 6.67 (d, *J*=8.98 Hz, 1 H) 7.11 - 7.22 (m, 4 H) 7.23 - 7.31 (m, 2 H) 7.34 (d, *J*=2.54 Hz, 1 H) 7.43 (d, *J*=7.22 Hz, 4 H) 7.47 - 7.55 (m, 3 H) 8.10 (dd, *J*=8.98, 2.34 Hz, 1 H) 8.31 (d, *J*=2.34 Hz, 1 H) 8.59 (d, *J*=2.15 Hz, 1 H). HPLC (6 min), *t<sub>R</sub>* = 1.41 min, HPLC purity >95%. LCMS (ESI) *m/z* 779 [M+H]<sup>+</sup>.

**4-[2-(1-Azetidin-3-yl-1H-pyrazol-5-yl)-4-chlorophenoxy]-3-cyano-N-1,3-thiazol-4-ylbenzenesulfonamide (59).** *tert*-butyl{[4-(4-chloro-2-{1-[1-(diphenylmethyl)azetidin-3-yl]-1H-pyrazol-5-yl}phenoxy)-3-cyanophenyl]sulfonyl}1,3-thiazol-4-ylcarbamate, (**58**) (224 mg, 0.287 mmol) was dissolved in dichloromethane (10 mL) and N,N,N',N'-tetramethylnaphthalene-1,8-diamine (150 mg, 0.70 mmol) was added, followed by 1-chloroethyl chloroformate (0.07 mL, 0.65 mmol) and the solution was stirred at room temperature for 3.5 hours. The mixture was concentrated in vacuo and the residue was dissolved in methanol (10 mL) and refluxed for 4 hours before concentrating in vacuo to give the crude title compound as a brown gum, as a mixture of 4-[2-(1-azetidin-3-yl-1H-pyrazol-5-yl)-4-chlorophenoxy]-3-cyano-N-1,3-thiazol-4-ylbenzenesulfonamide & *tert*-butyl ({4-[2-(1-azetidin-3-yl-1H-pyrazol-5-yl)-4-chlorophenoxy]-

1  
2  
3 3-cyanophenyl}sulfonyl)1,3-thiazol-4-ylcarbamate (200 mg crude). This mixture was stirred in  
4  
5 4M hydrogen chloride solution in 1,4-dioxane (10 mL) at room temperature for 2 hours. The  
6  
7 reaction mixture was concentrated in vacuo and the residue was partitioned between methyl-*t*-  
8  
9 butyl ether (80 mL) and water (40 mL) (neutralized to pH=7 with sodium hydrogen carbonate).  
10  
11 The organic layer was then concentrated in vacuo and the crude product purified by column  
12  
13 chromatography using dichloromethane:methanol:conc. ammonium hydroxide (90:10:1 to  
14  
15 70:30:3). This provided a buff powder (65 mg) which was triturated with methyl tert-butyl ether  
16  
17 to provide the title compound as a beige powder (55 mg, 33%). <sup>1</sup>H NMR (400 MHz, DMSO-*d*<sub>6</sub>)  
18  
19 δ ppm 4.00 - 4.12 (m, 4 H) 5.04 - 5.12 (m, 1 H) 6.28 (d, *J*=1.56 Hz, 1 H) 6.37 (s, 1 H) 6.84 (d,  
20  
21 *J*=8.97 Hz, 1 H) 7.41 (d, *J*=8.97 Hz, 1 H) 7.60 (dd, *J*=5.65, 2.14 Hz, 2 H) 7.67 (dd, *J*=8.78, 2.54  
22  
23 Hz, 1 H) 7.82 (dd, *J*=8.97, 1.95 Hz, 1 H) 7.99 (d, *J*=1.95 Hz, 1 H) 8.65 (d, *J*=2.34 Hz, 1 H).,  
24  
25 HPLC (2 min), *t*<sub>R</sub> = 1.26 min, HPLC purity >95%. LCMS (ESI) *m/z* 513 [M<sup>+</sup>H]<sup>+</sup>.  
26  
27  
28  
29  
30  
31  
32  
33

## 34 ASSOCIATED CONTENT

### 36 Supporting Information

37  
38 Detailed syntheses, characterization, purity analysis and molecular formula strings of all  
39  
40 compounds are disclosed. Electrophysiology protocols for ion channel in vitro profiling and  
41  
42 secondary pharmacology data is also outlined. This material is available free of charge via the  
43  
44 Internet at <http://pubs.acs.org>.  
45  
46  
47

### 48 Accession Code

49  
50 Coordinates and structure factors have been submitted to the PDB under accession code 5K7K  
51  
52 for compound **29** bound to CYP2C9. Authors will release the atomic coordinates and  
53  
54 experimental data upon article publication.  
55  
56  
57  
58  
59  
60

1  
2  
3  
4  
5  
6  
7  
8  
9  
10  
11  
12  
13  
14  
15  
16  
17  
18  
19  
20  
21  
22  
23  
24  
25  
26  
27  
28  
29  
30  
31  
32  
33  
34  
35  
36  
37  
38  
39  
40  
41  
42  
43  
44  
45  
46  
47  
48  
49  
50  
51  
52  
53  
54  
55  
56  
57  
58  
59  
60

AUTHOR INFORMATION**Corresponding Author**

\*To whom correspondence should be addressed. Tel +44 (0)1707 358693. E-mail:  
nigel.swain@heptares.com.

**Present Addresses**

† (N.A.S.) Heptares Therapeutics Ltd, BioPark, Broadwater Road, Welwyn Garden City, AL7  
3AX, United Kingdom. (R.I.S. and A.P.) AstraZeneca, Darwin Building, 310 Cambridge Science  
Park, Milton, Cambridge, CB4 0FZ, United Kingdom.

**Author Contributions**

The manuscript was written through contributions of all authors who have given approval for  
publication of the manuscript.

**Notes**

The authors declare no competing financial interest.

**ACKNOWLEDGMENT**

We acknowledge PeakDale Molecular (Concept Life Sciences) for synthetic support, Jill  
Chrencik for CYP2C9 structure PDB deposition and Rubben Torella for the CYP2C9 graphic.  
We also thank Raj Logan for the Pharmacokinetic, Dynamics and Metabolism screening support.

**ABBREVIATIONS**

ADME, Absorption Distribution Metabolism Excretion; AUC, area under curve; Boc, tert-butylloxycarbonyl;  $Cl_{int}$ , intrinsic clearance;  $C_{max}$ , maximum concentration;  $Cl_p$ , plasma clearance;  $Cl_u$ , unbound clearance; CYP, cytochrome P450; DDI, drug-drug interaction; DLM, dog liver microsomes; DMB di-methoxy benzyl; F, bioavailability;  $F_u$ , fraction unbound; HBA, H-bond acceptor; HBD, H-bond donor; hep, hepatocytes; HET, heterocycle; HLM, human liver microsomes; IV, intravenous; LHS, left hand side; LipE, lipophilic efficiency; MDCK-MDR1, Madin-Darby canine kidney, multi-drug resistance; OATP, organic anion-transporting polypeptide;  $P_{app}$ , apparent permeability; PK, pharmacokinetics; PPB, plasma protein binding; RHS, right hand side; RLM, rat liver microsomes; RRCK, Ralph Russ canine kidney; SAR, structure activity relationship;  $T_{1/2}$ , plasma half-life;  $T_{max}$ , time at maximum plasma concentration; TPSA, topological polar surface area;  $V_{ss}$ , volume of distribution (steady state).

## REFERENCES

- (1) (a) Goldin, A. L, Resurgence of sodium channel research. *Ann. Rev. Physiol.* **2001**, *63*, 871-894. (b) Wood, J. N.; Boorman, J. Voltage-gated sodium channel blockers; target validation and therapeutic potential. *Curr. Top. Med. Chem.* **2005**, *5*, 529-537.
- (2) (a) Bagal, S. K.; Brown, A. D.; Cox, P. J.; Omoto, K.; Owen, R. M.; Pryde, D. C.; Sidders, B.; Skerratt, S. E.; Stevens, E. B.; Storer, R. I.; Swain, N. A. Ion channels as therapeutic targets: a drug discovery perspective. *J. Med. Chem.* **2013**, *56*, 593-624. (b) Bagal, S. K.; Chapman, M. L.; Marron, B. E.; Prime, R.; Storer, R. I.; Swain, N. A.. Recent progress in sodium channel modulators for pain. *Bioorg. Med. Chem. Lett.* **2014**, *24*, 3690-3699.
- (3) Eijkelkamp, N.; Linley, J. E.; Baker, M. D.; Minett, M. S.; Cregg, R.; Werdehausen, R.; Rugiero, F.; Wood, J. N. Neurological perspectives on voltage-gated sodium channels. *Brain* **2012**, *135*, 2585-2612.



1  
2  
3  
4  
5  
6  
7  
8  
9  
10  
11  
12  
13  
14  
15  
16  
17  
18  
19  
20  
21  
22  
23  
24  
25  
26  
27  
28  
29  
30  
31  
32  
33  
34  
35  
36  
37  
38  
39  
40  
41  
42  
43  
44  
45  
46  
47  
48  
49  
50  
51  
52  
53  
54  
55  
56  
57  
58  
59  
60

(4) (a) Dib-Hajj, S. D.; Yang, Y.; Black, J. A.; Waxman, S. G. The Nav1.7 sodium channel: from molecule to man. *Nat. Rev. Neurosci.* **2013**, *14*, 49-62. (b) Waxman, S. G.; Zamponi, G. W. Regulating excitability of peripheral afferents: emerging ion channel targets. *Nat. Neurosci.* **2014**, *17*, 153-163. (c) Gingras, J.; Smith, S.; Matson, D. J.; Nye, D.; Couture, L.; Feric, E.; Yin, R.; Moyer, B. D.; Peterson, M. L.; Rottman, J. B.; Beiler, R. J.; Malmberg, A. B.; McDonough, S. I. Global Nav1.7 knockout mice recapitulate the phenotype of human congenital indifference to pain. *PLoS One* **2014**, *9*, e105895.

(5) (a) Cox J. J.; Reimann F.; Nicholas A. K.; Thornton, G.; Roberts, E.; Springell, K.; Karbani, G.; Jafri, H.; Mannan, J.; Raashid, Y.; Al-Gazali, L.; Hamamy, H.; Valente, E. M.; Gorman, S.; Williams, R.; McHale, D. P.; Wood, J. N.; Gribble, F. M.; Woods, G. C. An SCN9A channelopathy causes congenital inability to experience pain. *Nature* **2006**, *444*, 894-898. (b) Goldberg Y. P.; MacFarlane J.; MacDonald M. L.; Thompson J.; Dube, M. P.; Mattice, M.; Fraser, R.; Young, C.; Hossain, S.; Pape, T.; Payne, B.; Radomski, C.; Donaldson, G.; Ives, E.; Cox, J.; Younghusband, H. B.; Green, R.; Duff, A.; Bolthausen, E.; Grinspan, G. A.; Dimon, J. H.; Sibley, B. G.; Andria, G.; Toscano, E.; Kerdraon, J.; Bowsher, D.; Pimstone, S. N.; Samuels, M. E.; Sherrington, R.; Hayden, M. R. Loss-of-function mutations in the Nav1.7 gene underlie congenital indifference to pain in multiple human populations. *Clin. Genet.* **2007**, *71*, 311-319.

(6) (a) Fertleman C. R.; Baker M. D.; Parker K. A.; Moffatt S.; Elmslie, F. V.; Abrahamsen, B.; Ostman, J.; Kluqbauer, N.; Wood, J. N.; Gardiner, R. M.; Rees, M. SCN9A mutations in paroxysmal extreme pain disorder: allelic variants underlie distinct channel defects and phenotypes. *Neuron* **2006**, *52*, 767-774. (b) Yang Y.; Wang Y.; Li S.; Xu, Z.; Li, H.; Ma, L.; Fan, J.; Bu, D.; Fan, Z.; Wu, G.; Jin, J.; Ding, B.; Zhu, X.; Shen, Y. Mutations in SCN9A, encoding a sodium channel alpha subunit, in patients with primary erythralgia. *J. Med. Genet.*

1  
2  
3 **2004**, *41*, 171-174. (c) Drenth J. P.; te Morsche R. H.; Guillet, G.; Taieb, A.; Kirby, R. L.;  
4  
5 Jansen, J. B. SCN9A mutations define primary erythralgia as a neuropathic disorder of  
6  
7 voltage gated sodium channels. *J. Invest. Dermatol.* **2005**, *124*, 1333-1338.

8  
9  
10 (7) (a) Nardi, A.; Damann, N.; Hertrampf, T.; Kless, A. Advances in targeting voltage-gated  
11  
12 sodium channels with small molecules. *ChemMedChem.* **2012**, *7*, 1712-1740. (b) de Lera, R. M.;  
13  
14 Kraus, R. L. J. Voltage-gated sodium channels: Structure, function, pharmacology, and clinical  
15  
16 indications. *J. Med. Chem.* **2015**, *58*, 7093-7118. (c) King, G. F.; Vetter, I. No gain, no pain:  
17  
18 Nav1.7 as an analgesic target. *ACS Chem. Neurosci.* **2014**, *5*, 749-751.

19  
20  
21  
22  
23 (8) Beaudoin, S.; Laufer-Sweiler, M. C.; Markworth, C. J.; Marron, B. E.; Millan, D. S.;  
24  
25 Rawson, D. J.; Reister, S. M.; Sasaki, K.; Storer, R. I.; Stupple, P. A.; Swain, N. A.; West, C.  
26  
27 W.; Zhou, S. Sulfonamide derivatives. PCT Int. Appl. WO2010079443, Jul 15, 2010.

28  
29  
30  
31 (9) McCormack, K.; Santos, S.; Chapman, M. L.; Krafte, D. S.; Marron, B. E.; West, C. W.;  
32  
33 Krambis, M. J.; Antonio, B. M.; Zellmer, S. G.; Printzenhoff, D.; Padilla, K.; M.; Lin, Z.;  
34  
35 Wagoner, P. K.; Swain, N. A.; Stupple, P. A.; de Groot, M.; Butt, R. P.; Castle, N. A. Voltage  
36  
37 sensor interaction site for selective small molecule inhibitors of voltage-gated sodium channels.  
38  
39 *Proc. Natl. Acad. Sci. U. S. A.* **2013**, *110*, E2724-E2732.

40  
41  
42  
43  
44 (10) Ahuja, S.; Mukund, S.; Deng, L.; Khakh, K.; Chang, E.; Ho, H.; Shriver, S.; Young, C.; Lin,  
45  
46 S.; Johnson, J. P.; Wu, P.; Li, J.; Coons, M.; Tam, C.; Brillantes, B.; Sampang, H.; Mortara, K.;  
47  
48 Bowman, K. K.; Clark, K. R.; Estevez, A.; Xie, Z.; Verschoof, H.; Grinwood, M.; Dehnhardt, C.;  
49  
50 Andrez, J-C.; Focken, T.; Sutherlin, D. P.; Safina, B. S.; Starovasnik, M. A.; Ortwine, D. F.;  
51  
52 Franke, Y.; Cohen, C. J.; Hackos, D. H.; Koth, C. M.; Payandeh, J. Structural basis of Nav1.7  
53  
54 inhibition by an isoform-selective small-molecule antagonist. *Science* **2015**, *350*, 1491.

1  
2  
3 (11) Payandeh J.; Scheuer T.; Zheng N.; Catterall W. A. The crystal structure of a voltage-gated  
4 sodium channel. *Nature*, **2011**, *475*, 353-358.  
5  
6

7  
8  
9 (12) (a) Sun, S.; Cohen, C. J.; Dehnhardt C. M. Inhibitors of voltage-gated sodium channel  
10  $Na_v1.7$ : patent applications since 2010. *Pharm. Pat. Anal.* **2014**, *3*, 509-521. (b) Sun, S.; Jia, Q.;  
11 Zenova, A. Y.; Chafeev, M.; Zhang, Z.; Lin, S.; Kwan, R.; Grimwood, M. E.; Chowdhury, S.;  
12 Young, C.; Cohen, C. J.; Oballa, R. M.; The discovery of benzenesulfonamide-based potent and  
13 selective inhibitors of voltage-gated sodium channel  $Na_v1.7$ . *Bioorg. Med. Chem Lett.* **2014**, *24*,  
14 4397-4401. (c) Focken, T.; Liu, S.; Chahal, N.; Dauphinais, M.; Grimwood, M. E.; Chowdhury,  
15 S.; Hemeon, I.; Bichler, P.; Bogucki, D.; Waldbrook, M.; Bankar, G.; Sojo, L. E.; Young, C.;  
16 Lin, S.; Shuart, N.; Kwan, R.; Pang, J.; Chang, J. H.; Safina, B. S.; Sutherlin, D. P.; Johnson, Jr.  
17 J. P.; Dehnhardt, C. M.; Mansour, T. S.; Oballa, R. M.; Cohen, C. J.; Robinette, C. L. Discovery  
18 of aryl sulfonamides as isoform-selective inhibitors of  $Na_v1.7$  with efficacy in rodent pain  
19 models. *ACS Med. Chem. Lett.* **2016**, *7*, 277-282. (d) DiMauro, E. F.; Altmann, S.; Berry, L. M.;  
20 Bregman, H.; Chakka, N.; Chu-Moyer, M.; Bojic, E F; Foti, Robert S.; Fremeau, R.; Gao, H.;  
21 Gunaydin, H.; Guzman-Perez, A.; Hall, B. E.; Huang, H.; Jarosh, M.; Kornecook, T.; Lee, J.;  
22 Ligutti, J.; Liu, D.; Moyer, B. D.; Ortuno, D.; Rose, P. E.; Schenkel, L. B.; Taborn, K.; Wang, J.;  
23 Wang, Y.; Yu, V.; Weiss, M. M. Application of a parallel synthetic strategy in the discovery of  
24 biaryl acyl sulfonamides as efficient and selective  $Na_v1.7$  inhibitors. *J. Med. Chem.* **2016**, *59*,  
25 7818-7839. (e) Marx, I. E.; Dineen, T. A.; Able, J.; Bode, C.; Bregman, H.; Chu-Moyer, M.; Di  
26 Mauro, E. F.; Du, B.; Foti, R. S.; Fremeau, R. T.; Gao, H.; Gunaydin, H.; Hall, B. E.; Huang, L.;  
27 Kornecook, T.; Kreiman, C. R.; La, D. S.; Ligutti, J.; Lin, M. J.; Liu, D.; McDermott, J. S.;  
28 Moyer, B. D.; Peterson, E. A.; Roberts, J. T.; Rose, P.; Wang, J.; Youngblood, B. D.; Yu, V. L.;  
29 Weiss, M. M. Sulfonamides as selective  $Na_v1.7$  inhibitors: Optimizing potency and  
30  
31  
32  
33  
34  
35  
36  
37  
38  
39  
40  
41  
42  
43  
44  
45  
46  
47  
48  
49  
50  
51  
52  
53  
54  
55  
56  
57  
58  
59  
60

1  
2  
3 pharmacokinetics to enable in vivo target engagement. *ACS Med. Chem. Lett.* **2016**, *7*, 1062-  
4 1067. (f) Wu, Y.; Guernon, J.; Shi, J.; Ditta, J.; Robbins, K. J.; Rajamani, R.; Easton, A.;  
5  
6 Newton, A.; Bourin, C.; Mosure, K.; Soars, M. G.; Knox, R. J.; Matchett, M.; Pieschl, R. L.;  
7  
8 Post-Munson, D. J.; Wang, S.; Herrington, J.; Graef, J.; Newberry, K.; Bristow, L. J.; Meanwell,  
9  
10 N. A.; Olson, R.; Thompson, L. A.; Dzierba, C. Development of new benzenesulfonamides as  
11  
12 potent and selective Nav1.7 inhibitors for the treatment of pain. *J. Med. Chem.* **2017**, *60*, 2513-  
13  
14 2525. (g) Sparling, B. A.; Yi, S.; Able, J.; Bregman, H.; DiMauro, E. F.; Foti, R. S.; Gao, H.;  
15  
16 Guzman-Perez, A.; Huang, H.; Jarosh, M.; Kornecook, T.; Ligutti, J.; Milgram, B. C.; Moyer, B.  
17  
18 D.; Youngblood, B.; Yu, V. L.; Weiss, M. M. Discovery and hit-to-lead evaluation of piperazine  
19  
20 amides as selective, state-dependent Nav1.7 inhibitors. *Med. Chem. Commun.* **2017**, *8*, 744-754.  
21  
22 (h) Weiss, M. M.; Dineen, T. A.; Marx, I. E.; Altmann, S.; Boezio, A. A.; Bregman, H.; Chu-  
23  
24 Moyer, M. Y.; Di Mauro, E. F.; Bojic, E. F.; Foti, R. S.; Gao, H.; Graceffa, R. F.; Gunaydin, H.;  
25  
26 Guzman-Perez, A.; Huang, H.; Huang, L.; Jarosh, M.; Kornecook, T.; Kreiman, C. R.; Ligutti, J.;  
27  
28 La, D. S.; Lin, M. J.; Liu, D.; Moyer, B. D.; Nguyen, H. N.; Peterson, E. A.; Rose, P. E.; Taborn,  
29  
30 K.; Youngblood, B. D.; Yu, V. L.; Fremeau, R. T., Jr. Sulfonamides as selective Nav1.7  
31  
32 inhibitors: Optimizing potency and pharmacokinetics while mitigating metabolic liabilities. *J.*  
33  
34 *Med. Chem.* [Online early access]. DOI: 10.1021/acs.jmedchem.6b01851. Published Online: Mar  
35  
36 13, 2017. <http://pubs.acs.org/doi/abs/10.1021/acs.jmedchem.6b01851> (accessed Jun 14 2017). (i)  
37  
38 Graceffa, R. F.; Boezio, A. A.; Able, J.; Altmann, S.; Berry, L. M.; Boezio, C. M.; Butler, J. R.;  
39  
40 Chu-Moyer, M. Y.; Cooke, M.; Di Mauro, E. F.; Dineen, T. A.; Bojic, F. E.; Foti, R. S.;  
41  
42 Fremeau, R. T., Jr.; Guzman-Perez, A.; Gao, H.; Gunaydin, H.; Huang, H.; Huang, L.; Ilch, C.;  
43  
44 Jarosh, M.; Kornecook, T.; Kreiman, C. R.; La, D. S.; Ligutti, J.; Milgram, B. C.; Lin, M. J.;  
45  
46 Marx, I. E.; Nguyen, H. N.; Peterson, E. A.; Rescourio, G.; Roberts, J.; Schenkel, L. B.;  
47  
48  
49  
50  
51  
52  
53  
54  
55  
56  
57  
58  
59  
60

1  
2  
3 Shimanovich, R.; Sparling, B. A.; Stellwagen, J.; Taborn, K.; Vaida, K. R.; Wang, J.; Yeoman, J.  
4  
5 T. S.; Yu, V. L.; Zhu, D.; Moyer, B. D.; Weiss, M. M. Sulfonamides as selective  $\text{Na}_v1.7$   
6  
7 inhibitors: Optimizing potency, pharmacokinetics, and metabolic properties to obtain  
8  
9 atropisomeric quinolinone (AM-0466) that affords robust in vivo activity. *J. Med. Chem.* [Online  
10  
11 early access]. DOI: 10.1021/acs.jmedchem.6b01850. Published Online: Mar 21, 2017.  
12  
13 <http://pubs.acs.org/doi/abs/10.1021/acs.jmedchem.6b01850> (accessed Jun 14 2017).  
14  
15

16  
17  
18 (13) Stepan, A. F.; Walker, D. P.; Bauman, J.; Price, D. A.; Baillie, T. A.; Kalgutkar, A. S.; Aleo,  
19  
20 M. D. Structural alert/reactive metabolite concept as applied in medicinal chemistry to mitigate  
21  
22 the risk of idiosyncratic drug toxicity: a perspective based on the critical examination of trends in  
23  
24 the top 200 drugs marketed in the United States. *Chem. Res. Toxicol.* **2011**, *24*, 1345-1410.  
25  
26

27  
28  
29 (14) Castle, N.; Printzenhoff, D.; Zellmer, S.; Antonio, B.; Wickenden, A.; Silvia, C. Sodium  
30  
31 channel inhibitor drug discovery using automated high throughput electrophysiology platforms.  
32  
33 *Comb. Chem. High Throughput Screening* **2009**, *12*, 107-122.  
34  
35

36  
37 (15) Grime, K.; Paine, S. W. Species differences in biliary clearance and possible relevance of  
38  
39 hepatic uptake and efflux transporters involvement. *Drug Metab. Dispos.* **2013**, *41*, 372-378.  
40  
41

42  
43 (16) Jones, H. M.; Butt, R. P.; Webster, R. W.; Gurrell, I.; Dzygiel, P.; Flanagan, N.; Fraier, D.;  
44  
45 Hay, T.; Iavarone, L. E.; Luckwell, J.; Pearce, H.; Phipps, A.; Segelbacher, J.; Speed, B.;  
46  
47 Beaumont, K. Clinical micro-dose studies to explore the human pharmacokinetics of four  
48  
49 selective inhibitors of human  $\text{Na}_v1.7$  voltage-dependent sodium channels. *Clin. Pharmacokinet.*  
50  
51 **2016**, *55*, 875-887.  
52  
53  
54  
55  
56  
57  
58  
59  
60

(17) (a) Alexandrou, A. J.; Brown, A. R.; Turner, J.; Mis, M. A.; Wilbrey, A.; Payne, E. C.; Gutteridge, A.; Cox, P. J.; Butt, R. P.; Stevens, E. B.; Chapman, M. L.; Printzenhoff, D.; Lin, Z.; Marron, B. E.; West, C.; Castle, N. A.; Krafte, D.; Estacion, M.; Dib-Hajj, S. D.; Waxman, S. G.; Doyle, R.; Swain, N. A.; Storer, R. I.; Stupple, P. A.; Hounshell, J. A.; Rivara, M.; Patel, M. K.; Randall, A.. Subtype-selective small molecule inhibitors reveal a fundamental role for Nav<sub>v</sub>1.7 in nociceptor electrogenesis, axonal conduction and presynaptic release. *PLoS One*, **2016**, *11*, e0152405. (b) Theile, J. W.; Fuller, M. D.; Chapman, M. L., The selective Nav<sub>v</sub>1.7 inhibitor, PF-05089771, interacts equivalently with fast and slow inactivated Nav1.7 channels. *Mol. Pharm.* **2016**, *90*, 540-548.

Insert Table of Contents Graphic and Synopsis Here

